



Published in final edited form as:

*Adv Healthc Mater.* 2018 March ; 7(6): e1701024. doi:10.1002/adhm.201701024.

## Emerging Roles of Electrospun Nanofibers in Cancer Research

**Dr Shixuan Chen,**

Department of Surgery-Transplant and Mary & Dick Holland Regenerative Medicine Program,  
University of Nebraska Medical Center, Omaha, Nebraska 68198, United States

**Dr Sunil Kumar Boda,**

Department of Surgery-Transplant and Mary & Dick Holland Regenerative Medicine Program,  
University of Nebraska Medical Center, Omaha, Nebraska 68198, United States

**Prof Surinder K. Batra,**

Department of Biochemistry & Molecular Biology, University of Nebraska Medical Center, Omaha,  
Nebraska 68198, United States

**Prof Xiaoran Li, and**

Key Laboratory for Nano-Bio Interface Research, Division of Nanobiomedicine, Suzhou Institute  
of Nano-Tech and Nano-Bionics, Chinese Academy of Sciences, Suzhou, China

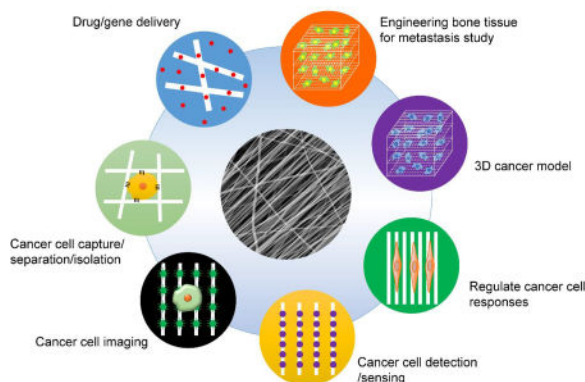
**Prof Jingwei Xie**

Department of Surgery-Transplant and Mary & Dick Holland Regenerative Medicine Program,  
University of Nebraska Medical Center, Omaha, Nebraska 68198, United States

### Abstract

This article reviews the recent progress of electrospun nanofibers in cancer research. It begins with a brief introduction to the emerging potential of electrospun nanofibers in cancer research. Next, a number of recent advances on the important features of electrospun nanofibers critical for cancer research are discussed including the incorporation of drugs, control of release kinetics, orientation and alignment of nanofibers, and the fabrication of 3D nanofiber scaffolds. This article further highlights the applications of electrospun nanofibers in several areas of cancer research including local chemotherapy, combinatorial therapy, cancer detection, cancer cell capture, regulation of cancer cell behavior, construction of *in vitro* 3D cancer model, and engineering of bone microenvironment for cancer metastasis. This Progress Report concludes with remarks on the challenges and future directions for design, fabrication, and application of electrospun nanofibers in cancer diagnostics and therapeutics.

### Graphic Abstract



This progress report reviews the application of electrospun nanofibers in cancer research, including drug/gene delivery, 3D cancer model, cancer cell detection/sensing, cancer cell imaging, cancer cell capture/separation/isolation, regulating the behavior of cancer cells, and engineering the pre-metastatic niche.

## 1. Introduction

Cancer, an intractable public health issue worldwide, has become the second leading cause of death in the United States.<sup>[1]</sup> Early cancer diagnosis and therapy remain unresolved healthcare challenges in spite of decades of laboratory and clinical research. In recent years, three-dimensional scaffolds are emerging as support matrices for 3D *in vitro* cancer models and drug delivery systems in cancer therapy. The *in vitro* cancer model has been employed as a platform for studies of drug discovery, drug toxicity, and anti-cancer mechanisms,<sup>[2]</sup> as well as cancer cell biology including cancer development, cancer cell motility in the metastasis, cell invasion, etc.<sup>[3]</sup> For *in vivo* cancer therapy, 3D scaffolds have widely served as implantable drug-releasing devices for local drug delivery.<sup>[4]</sup>

It is becoming increasingly clear that cancer cell monolayers on the 2D polystyrene surfaces do not reflect the essential feature of whole tumors, which are composed of multicellular tumor spheroids in 3D structures.<sup>[5]</sup> A variety of 3D scaffolds have been employed in engineering *in vitro* cancer model systems, including porous scaffolds<sup>[6]</sup>, self-assembled peptide hydrogels<sup>[7]</sup>, nanoparticles<sup>[8]</sup> and electrospun fibers<sup>[9]</sup>. Most of the *in vitro* systems are associated with undesirable microstructures and functions.<sup>[10]</sup> Among them, electrospun fibers with diameters ranging from nanometer to sub-micrometer, similar to collagen fibrils in the extracellular matrix (ECM) of tumors are considered to foster more intimate cell-cell and cell-matrix interactions.<sup>[11]</sup> In addition, the surface modification of electrospun fibers with ECM-derived proteins or peptides offers a closer resemblance to the tumor ECM.<sup>[12]</sup> The advances in electrospun fibers including drug encapsulation, surface modification, alignment and 3D fabrication lead to a rational design of 3D cancer models better mimicking the physiology and microenvironment of malignant tumors. The future research should be directed towards the construction of complex tissue structures and architectures with the aid of 3D printing technology.

For *in vivo* cancer therapy, nanoparticles administered through intravascular route are beneficial for the targeted delivery of therapeutic drugs.<sup>[13]</sup> However, their efficacy is restricted due to the short circulation time. Injectable hydrogels, which can be filled into the tumor site or cavity after surgical removal of solid tumor, allows for local drug delivery.<sup>[14]</sup> But hydrogels have major obstacles of substantial wash-out of the encapsulated drug during the long gelation time, and poor control over drug release profiles. Electrospun fibers allowing for topical drug release in a controlled and sustained manner would be suitable for cancer therapy with improved drug efficacy, reduced side effects and prolonged patients' life expectancy. Here, three possible applications of electrospun nanofibers in cancer therapeutics are listed. One application is that drug-loaded fibrous matrices are implanted into the tumor bed after magnetic resonance imaging (MRI)-assisted tumor localization.<sup>[15]</sup> Another application is that drug-loaded fibrous matrices are implanted into the post-operative tumor cavity immediately following resection of tumors, with the aim of killing residual tumor cells and inhibiting recurrence of tumors.<sup>[16]</sup> The third application is that drug-loaded fragmented nanofibers are intra-tumorally injected, which can be fabricated by cutting aligned electrospun fibers under cryogenic conditions.<sup>[17]</sup> In the future work, regenerative medicine should be combined with cancer therapies allowing simultaneous cancer suppression and tissue regeneration after resection of tumors.

The existing reviews on applications of electrospun nanofibers in cancer study mainly focus on drug/gene delivery, which may not fully reflect the advantages and applications of electrospun nanofibers in cancer-related research. Therefore, in the present Progress Report, we highlight the applications of electrospun nanofibers in cancer research including anti-cancer drug/gene delivery<sup>[18]</sup>, 3D *in vitro* cancer model<sup>[19]</sup>, cancer cell detection/sensing<sup>[20]</sup>, cancer cell imaging<sup>[21]</sup>, cancer cell capture/separation/isolation<sup>[22]</sup>, regulation of cancer cell behavior<sup>[23]</sup> and engineering bone tissue for metastasis study<sup>[24]</sup>. This review concludes with remarks on the challenges and future directions for the design, fabrication, modification and applications of electrospun nanofibers in cancer research.

## 2. Recent Progress in Electrospun Nanofibers

### 2.1. Incorporation of drugs

The electrospun nanofibers were used for the first time in drug delivery by Kenawy *et al.* in 2002.<sup>[25]</sup> From 2002 till date, electrospun nanofiber membranes have been widely explored as carriers for the delivery of various drugs owing to their unique features including ease of drug incorporation during electrospinning, large surface area to volume ratio, highly porous and interconnected architecture, and tailorable material properties. The flexibility in material properties, arise from the high versatility in polymer composition, fiber diameter, porosity, morphology, and ease of surface functionalization. All the above parameters permit a strong control over drug release profiles.<sup>[26]</sup> Up to date, a variety of therapeutic agents, ranging from small molecule drugs to large biomacromolecules such as antibiotics, proteins, DNA or siRNA, oligo/polypeptides have been successfully incorporated into electrospun nanofibers. Table 1 lists the representative anticancer drug, gene, and virus encapsulation into electrospun nanofibers with varied polymer compositions. However, it is important to note that up to date, all the electrospun nanofiber-based systems for cancer research are still

in preclinical studies/trials only. Figure 1A shows the two typical methods for drug incorporation into electrospun nanofibers including simultaneous encapsulation and surface modification for cancer research. Encapsulation of anti-cancer drugs/genes is mainly for therapeutic applications, while surface modification with proteins or growth factors is for the establishment of 3D *in vitro* cancer models and surface immobilization of specific species is for cancer cell detection/sensing and cancer cell capture/separation/isolation. Their corresponding release mechanisms are shown in Figure 1B.

**2.1.1. Encapsulation**—Encapsulation provides a straightforward method for one-step immobilization of drugs and bioactive agents. The simplest way for drug encapsulation within electrospun nanofibers is direct electrospinning of a blend of drug and polymer solution through a single nozzle. However, the loading capacity and distribution uniformity of the encapsulated drug in electrospun fibers are largely dependent on the drug solubility and compatibility in the polymer solution.<sup>[46]</sup> The general solubility principle based on ‘like dissolves like’ is that hydrophobic drugs like paclitaxel (PTX) and hydrophilic drugs like doxorubicin hydrochloride (DOX) can be readily encapsulated in hydrophobic polymers and hydrophilic polymers, respectively. However, the hydrophilic drugs can also be encapsulated in hydrophobic polymers using the following strategies: co-axial electrospinning<sup>[47]</sup>, mixing the drug powders in the polymer solution<sup>[48]</sup>, and emulsion electrospinning<sup>[49]</sup>.

Simultaneous encapsulation of hydrophobic and hydrophilic drugs in a single device provides a new paradigm for combination therapy in cancer treatment, which can elicit synergistic therapeutic effect and reduce toxicity. Emulsion electrospinning provides a straightforward approach for simultaneous encapsulation of hydrophilic and hydrophobic drugs in nanofibers due to the formation water-in-oil (W/O) or oil-in-water (O/W) emulsion with hydrophilic drugs in the aqueous phase and hydrophobic drugs in the oily phase.<sup>[32]</sup> A breakthrough in encapsulation based on electrospinning is to use a co-axial or tri-axial nozzle setup for loading hydrophilic and hydrophobic drugs in separate layers of compatible polymers or in the same layer of core-sheath or multi-layered nanofibers.<sup>[50]</sup> Incorporation of drug-loaded nanospheres into electrospun fibers is another strategy for drug encapsulation in order to prolong the duration of drug release.<sup>[51]</sup>

**2.1.2. Surface immobilization**—Surface modification post-electrospinning including simple physical adsorption<sup>[52]</sup>, surface coating through electrostatic interaction<sup>[53]</sup>, polymerization<sup>[54]</sup>, mineralization<sup>[55]</sup>, atomic layer deposition<sup>[56]</sup>, layer-by-layer deposition<sup>[57]</sup>, and surface conjugation through hydrogen bond, ionic bond, and/or covalent bond<sup>[58]</sup>. All these surface modification methods allow for the immobilization of drugs onto the nanofiber surface without impairing the fiber properties and drug bioactivity<sup>[59]</sup>. Surface immobilization was rarely used for incorporating small-molecule anticancer drugs because of the fast release kinetics. In contrast, it is ideal for immobilization of biologics owing to a better preservation of their bioactivity since the post-electrospinning modification avoids exposure to organic solvent and destabilizing conditions during the electrospinning process. Ebara *et al.* reported the immobilization of an inactivated sendai virus to electrospun poly ( $\epsilon$ -caprolactone) (PCL) nanofibers for cancer therapy<sup>[44]</sup>. The inactivated sendai virus induces tumor specific apoptosis and anti-cancer immunity *in vitro* and *in vivo*<sup>[60]</sup>. In their work,

PCL electrospun nanofibers were first deposited with poly-L-Lysine (PLL) and alginic acid in a layer-by-layer fashion, and then the sendai virus was immobilized to the outermost cationic PLL surface. The release of sendai virus reached equilibrium at around 60 hemagglutinin unit (HAU) after 8 h, which was sufficient to induce the cytotoxicity of metastatic prostate cancer PC-3 cells. Besides chemotherapy, hyperthermia treatment provides an attractive method to complement the conventional therapies. As an illustrative example, Fe<sub>3</sub>O<sub>4</sub> nanoparticles were deposited on the surface of electrospun chitosan nanofibers by immersing the nanofibers in Fe<sup>+2</sup>/Fe<sup>+3</sup> solution to initiate chemical co-precipitation.<sup>[45]</sup> The heat generated by the magnetic composite nanofibers inhibited cancer cell proliferation upon application of an oscillating magnetic field. Compared with drug encapsulation which is a simple strategy for sustained release, surface modification with bioactive substances renders electrospun nanofibers with more functions. For example, the conjugation of peptides, antibodies, and ligands to electrospun nanofibers have been demonstrated to be effective in cancer cell detection and cancer cell capture.

## 2.2. Controlled Release

**2.2.1. Microstructure controlled release**—The microstructure refers to the fine inner structure of a single nanofiber, which plays an essential role in controlled drug release. A variety of microstructures presented in a single fiber including homogenous structure, core-sheath structure<sup>[61]</sup>, and multilayered structure<sup>[62]</sup> have been explored with the aid of blend, emulsion, coaxial, tri-axial and multi-axial electrospinning (Figure 2A). Electrospinning of a drug/polymer blend offers a simple way for homogeneously loading drugs in fibers. Unfortunately, the method is often associated with a severe burst release, resulting in a high initial dose and reduced effective lifetime<sup>[63]</sup>. The development of secondary microstructures such as core-sheath and multilayered structure is of crucial importance to avoid the initial burst release. The core-sheath structured nanofibers usually display more sustained release profiles compared to the blended nanofibers. Electrospinning of emulsion generates core-sheath structured nanofibers with lower burst release, but still exhibit a small initial burst release.<sup>[64]</sup> By utilizing coaxial electrospinning, individual components are simultaneously electrospun through separate feeding channels to produce core-sheath structured nanofibers.<sup>[65]</sup> Not surprisingly, the existence of sheath may reduce the burst release, and prolong the drug release from the core portion.<sup>[66]</sup> It is worth mentioning that the core-sheath structured nanofiber provides a powerful depot for controlled release of water-soluble drugs and bioactive agents, such as DNA and RNA. Moreover coaxial electrospinning is capable of encapsulating dual drugs simultaneously, with one in the coaxial nanofiber core, and the other in the sheath region.<sup>[67]</sup>

Generally, hydrophobic polymers are employed as the sheaths in coaxial electrospinning. However, biocompatible hydrophilic polymers, such as gelatin, collagen and hyaluronic acid (HA) are preferred for tissue engineering. Tri-axial electrospinning is a step further with the development of a three-layer microstructure composed of core, intermediate and sheath region.<sup>[68]</sup> The three-layered structure is particularly important when using a hydrophilic material as the sheath in order to obtain excellent biocompatibility. Steckl *et al.* presented a dual drug delivery system using tri-axial structured nanofibers, in which the core region consisted of one drug and poly(vinylpyrrolidone) (PVP), the intermediate region consisted

of PCL, and the sheath region consisted of the second drug and hygroscopic layer. With the intermediate layer as a buffer region between the inner core and the outer sheath, a  $\sim 24\times$  slower release than that from coaxial fibers was achieved. Meanwhile, the hygroscopic layer provided an initial burst release of  $\sim 80\%$  within one hour duration.<sup>[50]</sup>

Moreover, the introduction of nanospheres/micelles into the core-sheath structure ensures a hierarchical architecture. As an example, active-targeting micelles were encapsulated in core-sheath structured nanofibers by coaxial electrospinning with a mixture of poly(vinyl alcohol) (PVA) and the micelles as the core component and cross-linked gelatin as the sheath layer. As compared with the commonly used delivery strategy of repeated intravenous injection of micelles for cancer therapy, the implantable DOX loaded micelle-in-nanofiber device could reduce the frequency of drug administration, drug dose and side effects, while maintaining high therapeutic efficacy against artificial solid tumor.<sup>[29h]</sup> Encapsulation of micelles into electrospun nanofibers can enhance the stability of micelles and confer longer period of sustained release compared to micelle formulations. However, a uniform dispersion of micelles in the polymer solution is often the key issue during the electrospinning of polymer-micelle mixtures.

**2.2.2. Macrostructure controlled release—**The macrostructure refers to the integral structure of nanofiber-based drug release device, which exerts a high degree of control over drug release kinetics. The simplest strategy is to manually stack nanofiber mats/membranes/meshes to form a multi-layered 3D structure. The nanofiber layer without incorporating drugs could provide a physical barrier to prevent water penetration and thus retard drug release from the other drug-incorporated nanofiber layers. Based on this strategy, Grinstaff *et al.* developed a tri-layered electrospun nanofiber device composed of an anticancer drug SN-38-loaded central core layer, between two “shield” layers of mesh without drug and resistant to solvent wetting.<sup>[69]</sup> The tri-layered device displayed a markedly delayed and prolonged kinetics with a slow initial release over 10 days, followed by a sustained release over 30 days. The extended cytotoxicity results of the tri-layered device on Lewis Lung Carcinoma (LLC) cells over 20 days confirmed sustained drug release. In a similar work, the asymmetric multilayer polylactide nanofiber meshes were used to prolong the release of oxaliplatin for prevention of liver cancer recurrence after surgery in mice.<sup>[70]</sup> Notably, by alternatively stacking the nanofiber membranes/meshes with and without incorporation of drugs, the sequential release of multiple drugs can be achieved.<sup>[71]</sup> As shown in Figure 2B, the device was composed of 4 layers: 1) first drug-loaded mesh, 2) barrier mesh, 3) second drug-loaded mesh and 4) basement mesh. The *in vitro* release results demonstrated that the first drug was released rapidly within the first 30 min, without leakage of the second drug, followed by a steady release of the second drug after 1 h due to hindrance of the barrier mesh. Another similar study also demonstrated time-programmed dichloroacetate and oxaliplatin release by multilayered nanofiber mats in the prevention of local cervical carcinoma recurrence following surgery.<sup>[72]</sup> The time-programmed dual release system may be used for advanced multidrug combination therapy as it could overcome the chemoresistance caused by a single drug. However, several issues remain unresolved with the aforementioned multilayered nanofiber stacks. These devices, which are mainly formed by manually stacking, pose difficulties in the scale-up manufacturing process. Also, the



stacked meshes mainly provide a physical barrier only from the top or bottom surface but not from the lateral sides, which can pose problems for the precise control of drug release.

**2.2.3. Composition controlled release**—Besides the microstructure of nanofibers and macrostructure of nanofiber-based devices, the composition of nanofibers provides a fundamental basis for tailoring drug release kinetics. Natural polymers, synthetic polymers, and polymer blends have been extensively electrospun into nanofibers for drug delivery.<sup>[73]</sup> The chemistry of the nanofibers, which is the determining factor in wetting behavior and degradation rate plays a dominant role in controlling drug release. The additives (e.g., hydrophobic and hydrophilic materials) to electrospun nanofibers significantly affect the wetting behavior, resulting in regulation of drug release from nanofibers. For example, Grinstaff *et al.* synthesized a superhydrophobic material poly(glycerol monostearate-*co*-ε-caprolactone) (PGC-C18) as a doping agent to electrospun PCL nanofiber meshes to tune the anticancer drug release rate.<sup>[74]</sup> The cumulative release of anticancer agent SN-38 from 10% PGC-C18 doped electrospun PCL nanofiber meshes was more than 60% within 9 weeks. Meanwhile only 10% of SN-38 was released from both 30% and 50% PGC-C18 doped electrospun PCL nanofiber meshes. In their follow-up study, they utilized 30% PGC-C18 doped electrospun PCL nanofiber meshes for cisplatin encapsulation, and a linear sustained release over ~90 days was achieved. Notably less than 1% of cisplatin release was recorded within 24 h, as compared to >95% of cisplatin release from pure PCL nanofiber meshes within the same period of time. The *in vivo* evaluation demonstrated a remarkable increase in the median recurrence-free survival to >23 days, when compared to standard intraperitoneal cisplatin therapy of equivalent dose (Figure 2C).<sup>[28b]</sup> On the other hand, the addition of hydrophilic materials such as poly(ethylene glycol) (PEG) enhanced water uptake of the electrospun fibers, and subsequently accelerated drug release.<sup>[75]</sup>

The aforementioned devices usually offer sustained drug release, but with limited control over release rate, relying on the passive diffusion of drugs from the electrospun fibers. Intriguingly, the use of stimuli-responsive polymers enables on-demand release of encapsulated drugs because the polymer can sense and respond to signals and variations in the surrounding environment, leading to microstructure change and drug release.<sup>[76]</sup> These stimuli include: 1) physical stimuli, such as temperature, ultrasound, light, magnetic field and mechanical stress, 2) chemical stimuli, such as pH and ionic strength, and 3) biological stimuli, such as enzyme and biomolecules.<sup>[77]</sup> The thermo-responsive drug delivery system is the most studied stimuli-triggered release system for cancer therapy. Ideally, the device should retain the drugs at body temperature of 37 °C, and rapidly deliver the drug under hyperthermic conditions (40–42 °C). Thermal-responsive DOX-loaded liposomes have achieved translation into clinical trials (ThermoDOX).<sup>[78]</sup> Alternatively, the inclusion of thermo-responsive materials in the nano/ microfibrinous scaffolds may provide an on-demand and regional drug delivery. As an example, Aoyagi *et al.* reported a smart hyperthermia electrospun nanofiber with switchable drug release to induce cancer apoptosis.<sup>[29g]</sup> Magnetic nanoparticles (MNPs), as the source of heat, and anticancer drug DOX were encapsulated into nanofibers composed of temperature-responsive copolymer of NIPAAm and N-hydroxymethylacrylamide (HMAAm). The DOX/MNP electrospun fibers led to 70% death of human melanoma cells with exposure to 5 min of alternating magnetic field due to a

synergistic effect of chemotherapy and hyperthermia. In general, the application of a thermo-responsive delivery system is hampered by the limited sensitivity to respond to slight temperature fluctuations at the physiological temperature. Apart from thermo-responsive systems, external stimuli in the form of ultrasound and electric fields have been utilized to regulate drug release. In the former case, high-intensity focused ultrasound (HIFU), which has been used clinically in uterine fibroid treatment, has been employed in triggering drug delivery. For example, Grinstaff *et al.* prepared superhydrophobic fibrous mesh composed of PCL and PGC-C18, in which air is entrapped both at the surface and within the 3D structure.<sup>[79]</sup> The HIFU treatment could trigger the release of SN-38 attributed to the removal of air layer by the pressure wavefront. In the latter scenario, electric field-responsive drug carriers have been developed using electroactive polymers. The electrical field can lead to swelling, bending, or shrinking of the drug carrier, allowing for controlled drug release. Kim *et al.* prepared electro-responsive drug carriers by electrospinning of PVA/poly(acrylic acid) (PAA)/multi-walled carbon nanotubes (MWCNTs) composites. The application of electric field increased drug release significantly, and higher electric voltages induced faster drug release.<sup>[80]</sup> In a different study, Xie *et al.* developed a pH-responsive drug delivery device based on polydopamine-coated PCL electrospun fibers owing to the selective permeability of polydopamine coating for charged molecules at various pH values.<sup>[29f]</sup> It was found that the composite fibers released DOX in acidic aqueous solution, rather than in neutral and basic aqueous solution, resulting in a dramatic decrease in cancer cell viability.

The stimuli-responsive delivery system offers the promise of precise therapy against cancer cells avoiding damage to normal healthy tissues, arising from the control of drug release at specific times and locations. However, although the proof of concept has been successfully demonstrated *in vitro*, few studies have been carried out *in vivo*. The complexity of system design, introduction of non-degradable materials, and low penetration depth of the externally applied stimuli are among the major challenges which need to be addressed.

**2.2.4. Drug release mechanism**—The mechanism of drug release from electrospun fibers is mainly related to drug diffusion, drug dissolution, drug adsorption-desorption, and polymer erosion/degradation. Generally, the drug release follows diffusion-controlled kinetics for non-degradable polymers<sup>[81]</sup>, degradation-controlled kinetics for fast degradable polymers<sup>[82]</sup>, and combined kinetics of diffusion and degradation for slowly degradable polymers<sup>[83]</sup>. The drug release kinetics from electrospun fibers is mainly influenced by the polymer composition<sup>[25]</sup>, polymer crystallinity<sup>[83]</sup>, drug solubility in polymer<sup>[84]</sup>, drug distribution in fiber<sup>[85]</sup>, drug-polymer interaction<sup>[86]</sup>, and fiber size and morphology<sup>[87]</sup>. Typically, the electrospun fiber formulations share the feature of a classical biphasic drug release pattern with a burst release at the initial stage followed by a sustained release. For electrospinning of blended drug and polymers, drug enrichment at the fiber surface occurs, resulting in a high burst release. To better control the drug release, core-sheath structured fibers prepared by co-axial/tri-axial electrospinning have been developed, and a delayed and prolonged release has been achieved because of the sheath barriers. Extended drug release from the core-sheath structured fibers follows zero-order kinetics with no burst release, an ideal release model for long-term controlled drug release<sup>[88]</sup> Viry *et al.* reported a nearly linear release of small-molecule drugs over 18 days from core-sheath structured fibers



prepared by a combination of emulsion and coaxial electrospinning. In contrast, a 4-day linear release followed by a consistent, steady release for core-sheath fibers prepared by coaxial electrospinning alone was recorded.<sup>[89]</sup>

With respect to cancer therapy, pH-triggered release kinetics has been reported due to the acidic microenvironment of the tumor tissue, with reduction in pH value from 7.4 (normal tissue) to 6.8 (cancerous tissue). As a proof of concept, Cui *et al.* developed electrospun poly(L-lactic) (PLLA) fibers loaded with CaCO<sub>3</sub>-capped DOX-mesoporous silica nanoparticles (MSN).<sup>[29e]</sup> When the composite fibers encounter protons (H<sup>+</sup>) from the acids released by the tumor cells, CaCO<sub>3</sub> reacts with H<sup>+</sup> to produce CO<sub>2</sub> gas, enabling water penetration into the PLLA fibers, and facilitating the drug release. As expected, the amount of DOX released from PLLA-MSN-DOX-CaCO<sub>3</sub> composite fibers increased significantly as pH decreased, and 10%, 60%, and 100% of DOX was released after 40 days of incubation at pH 7.4, pH 5.0, and pH 3.0, respectively.

Mathematical models have been developed to describe drug release from one-dimensional materials in different scenarios. A one-dimensional drug diffusion model under perfect sink conditions for the transport of drugs from non-swellable devices is best described by the following equation.<sup>[90]</sup>

$$\frac{M_t}{M_\infty} = a_0 + kt^n$$

where  $M_t$  is the mass of drug released at time  $t$ ,  $M_\infty$  is the mass of drug released as time approaches infinity (or equivalently the total amount of drug encapsulated),  $a_0$  is a constant representing the percentage of burst release,  $k$  is a constant, and  $n$  is the diffusional exponent, which is an index for the transport mechanism. For one-dimensional Fickian diffusion of drugs from mono-dispersed cylinders,  $n$  is 0.45. In a different study, a desorption model is described by the following equation.<sup>[91]</sup>

$$\frac{M_t}{M_\infty} = \alpha \left[ 1 - \exp\left(-\frac{\pi^2}{8} \frac{t}{\tau_r}\right) \right]$$

where  $M_t$  is the mass of drug released at time  $t$ ,  $M_\infty$  is the mass of drug released as time approaches infinity (or equivalently the total amount of drug encapsulated),  $\alpha$  is nanoporosity factor, and  $\tau_r$  is the characteristic time. For the core-shell nanofibers (with blended core or monolithic core), the core contains water-soluble pluronic F-127 surfactant, the latter leaches out in parallel with the drug release process creating more pores. The two-stage drug release on time is described by the following equation.<sup>[92]</sup>

$$\frac{M_t}{M_\infty} = \alpha_1 \left[ 1 - \exp\left(-\frac{\pi^2}{8} \frac{t}{\tau_{r1}}\right) \right] + \alpha_2 \left[ 1 - \exp\left(-\frac{\pi^2}{8} \frac{t}{\tau_{r2}}\right) \right]$$

where  $\alpha_1$  and  $\tau_{r1}$  denote the nanoporosity factor and the characteristic time of drug release from the pre-existing pores, respectively and  $\alpha_2$  and  $\tau_{r2}$  denote the nanoporosity factor and

the characteristic time of drug release driven by pluronic F127 leaching, respectively. A separate work attempted to estimate the impact of structural parameters on drug release from the nanofiber mats using a two dimensional finite element numerical model.<sup>[93]</sup> It was found that for the same materials with similar porosity, the drug release from mats consisting of aligned fibers is slower than that of random fibers. In a further study, this model based on the diffusion effective coefficients and sorption process was used to describe drug release from nanofiber meshes in the PBS solution and PVA hydrogel.<sup>[94]</sup> The results from the numerical model were in agreement with the experimental drug release data.

### 2.3. Alignment

The flexibility in nanofiber assemblies has broadened their applications effectively, and up to date, a number of fiber assemblies including randomly-oriented, uniaxially-aligned, and radially-aligned structures have been successfully developed. In principle, fiber alignment can be achieved either through mechanical force or electric field. For the nanofiber assemblies, making use of different collectors is a simple way to control the fiber alignment. For example, the random fiber is generally collected on a metal plate<sup>[95]</sup>. The aligned fibers can be deposited on a high-speed rotating drum<sup>[96]</sup> or two conductive substrates separated by a void gap<sup>[97]</sup>. Alternatively, the fast moving 2D substrates can be used to write fiber patterns based on low-voltage electrospinning.<sup>[98]</sup> Nanofiber mats with square arrayed microwells can be fabricated using patterned metal beads.<sup>[99]</sup> The radially-aligned fibers can be prepared by utilizing a collector composed of a central point electrode and a peripheral ring electrode.<sup>[100]</sup> Randomly oriented nanofibers are capable of mimicking the ECM architecture of tumor tissue, and have been widely applied for the design of 3D cancer models<sup>[101]</sup> and biosensors for cancer cell detection,<sup>[102]</sup> capture and isolation<sup>[103]</sup>. In contrast with random nanofibers, the aligned feature greatly endows enhanced capabilities in regulating cancer cell behavior including cancer cell proliferation, migration and invasion<sup>[104]</sup>, gene expression<sup>[105]</sup>, and signal transduction<sup>[106]</sup>.

### 2.4. 3D Fabrication

There is an imperative need for the development of 3D electrospun nanofiber scaffolds resembling the spatial architecture of natural ECM. The simplest method for fabricating 3D mats with certain thickness is to directly deposit electrospun nanofibers on the collector for a sufficiently large period of time.<sup>[15]</sup> However, the inherent drawback of small pore size preventing cell infiltration has dramatically limited the application of electrospun nanofiber mats.<sup>[107]</sup> Hence, many attempts have been made to develop 3D scaffolds with high porosity.<sup>[107–108]</sup> Towards this end, various approaches are being developed. For instance, electrospun fibers can be assembled into 3D scaffolds with cellular architecture through freeze-drying of solutions containing short electrospun nanofibers (Figure 3A).<sup>[109]</sup> By using this method, Mo *et al.* fabricated poly(lactic acid) (PLA)/gelatin nanofiber-assembled 3D scaffolds, and demonstrated that L-929 cells proliferated and infiltrated into the 3D scaffolds, with cell movement from one side of scaffold to the other side.<sup>[110]</sup> Similarly, Park *et al.* utilized a cold plate as the collector to produce crystallized silk fibroin nanofibers, followed by freeze-drying for 3D scaffold construction.<sup>[111]</sup> The aforementioned 3D electrospun nanofiber scaffolds provide potential candidates to overcome the intrinsic shortcoming of 2D nanofiber mats. However, most of the studies have been limited to the

fabrication of 3D scaffolds composed of random nanofibers and/or certain materials. The resultant scaffolds often have insufficient thickness, restricted geometries, and/or uncontrolled porosity. These fabricated scaffolds are also associated with disordered structures and lack of nanotopographic cues, which is not conducive for cell migration. Recently, Xie *et al.* developed 3D nanofiber scaffolds by expanding 2D electrospun nanofiber membranes via a modified gas-foaming technique, in which hydrolysis of 1 M sodium borohydride was used to generate hydrogen gas bubbles.<sup>[112]</sup> Subsequently, the expanded nanofiber scaffolds were freeze-dried to maintain their integrity. It was found that the porosity of expanded 3D nanofiber scaffold increased to > 99% (Figure 3B). This strategy is capable of making 3D nanofiber scaffolds with maintenance of aligned nanotopographic cues. More recently, Xie *et al.* fabricated expanded nanofiber scaffolds with increased area and precise control of thickness using a customized mold during the expansion and freeze-drying process.<sup>[113]</sup> In earlier studies, Xie *et al.* also reported a straightforward approach for preparing 3D scaffolds in a basket-weaved structure composed of fine electrospun nanofiber stripes. Specifically, the prepared aligned electrospun membrane was cut into fine stripes along the direction of fiber alignment, and then the stripes were weaved by making use of 'noobing' technique to form a desired 3D architecture, whose edges were sealed via thermal treatment (Figure 3C).<sup>[114]</sup> Lastly, a combination of direct polymer melt deposition and electrospinning provides a robust method for the development of a 3D fashioned ECM-like structure composed of microfibers and nanofibers, in which nanofibers produced by electrospinning were deposited on the surface of microfibers generated by direct polymer melt deposition (Figure 3D).<sup>[115]</sup>

### 3. Emerging Roles of Electrospun Nanofibers in Cancer Research

#### 3.1. Drug/Gene Delivery

**3.1.1. Single drug delivery**—Up to now, chemotherapy and its combination are the most accepted and effective treatment for cancer treatment. One of the major problems for cancer chemotherapy is the side effects, resulting in a fatal damage to non-tumorigenic healthy proliferating cells.<sup>[116]</sup> Due to the alleviation of side effects and ease of reaching effective concentrations, electrospun nanofibers have been widely explored as an implant for local sustained anticancer drug delivery to the tumor site. Wu *et al.* utilized PLLA electrospun nanofibers as carrier for titanocene dichloride delivery against lung tumor cells, with 11.2%, 22.1%, 44.2% and 68.2% of human lung tumor cell growth inhibition for different titanocene dichloride loadings (40, 80, 160 and 240 mg/L) into the fiber mats.<sup>[36]</sup> Jing *et al.* prepared doxorubicin-loaded PLLA electrospun nanofibers for the inhibition of unresectable liver cancer and prevention of post-surgery tumor recurrence. Notably, an increase in the median survival time from 14 days to 38 days was achieved in the mice bearing secondary hepatic carcinoma.<sup>[29d]</sup> Koyakutty *et al.* utilized a temozolomide loaded poly(lactic-co-glycolic acid)(PLGA)/PLA/PCL electrospun mat for the treatment of recurrent glioma.<sup>[15]</sup> The drug loaded nanofiber mats after implantation to the resected orthotopic rat glioma exhibited a constant drug release rate (116.6 µg/day) with negligible leakage into the peripheral blood (<100 ng). Further, the one month-releasing implants led to the long term (>4 month) survival of > 85% rats.

**3.1.2. Multi-drug delivery**—Generally, a single anticancer drug delivery system may not be sufficient for clinical applications, as the single drug can often lead to the development of chemoresistance after prolonged use. Hence, multiple drug delivery systems are required to improve the therapeutic efficacy owing to a synergistic effect acted by different therapeutic agents. This may help overcome the chemoresistance caused by single drug. In a related study, two anticancer drugs designated CPT-11 and SN-38 were encapsulated in 10% PGC-C18 doped PCL electrospun mesh. A prolonged release over 90 days of CPT-11 and SN-38 was achieved, resulting in significant tumor cytotoxicity against a human colorectal cell line (HT-29).<sup>[27]</sup> More importantly, core-sheath structured fibers prepared by emulsion electrospinning and coaxial electrospinning offer excellent drug carrier options for multiple drug delivery. To this end, Jing *et al.* employed emulsion electrospinning to simultaneously encapsulate hydrophobic drug PTX and hydrophilic drug DOX into poly(ethylene glycol)-poly(L-lactic acid) (PEG-PLA) nanofiber mats.<sup>[32]</sup> The dual drug-loaded fibers displayed a quick release of DOX followed by a sustained release of PTX, leading to a higher inhibition and apoptosis against rat glioma C6 cells in comparison to a single drug delivery system. In addition, sequential delivery of different drugs can elicit pronounced antitumor efficacy. For example, the sequential delivery of vascular disrupting agent combretastatin A-4 and chemotherapeutic drug hydroxycamptothecin from electrospun nanofibers prepared by emulsion electrospinning caused a sequential killing of endothelial and tumor cells, while the *in vivo* study results indicated a significant antitumor efficacy, tumor vasculature destruction, and minimal tumor metastasis to the lung.<sup>[35]</sup>

However, the emulsion electrospinning may involve the emulsifier component with poor biocompatibility, and coaxial electrospinning usually needs substantial optimization of fabrication parameters. Therefore, nano- and microscale vehicles such as nanoparticles have been incorporated into electrospun fibers for multidrug delivery. For a notable example, hydrophilic drug DOX loaded mesoporous zinc oxide (ZnO) nanospheres and hydrophobic drug camptothecin were mixed with a PLGA/gelatin solution prior to electrospinning for the fabrication of dual drug loaded electrospun hybrid nanofibers, which showed strong antitumor efficacy against HepG-2 cells.<sup>[30]</sup> In a separate study, Li *et al.* presented a hydrophilic-hydrophobic dual drug delivery system by electrospinning of poly(ethylene oxide) (PEO) containing vehicles constructed by mixed surfactant cetyltrimethylammonium bromide (CTAB)/sodium dodecylbenzenesulfonate (SDBS).<sup>[117]</sup> The hydrophilic anticancer model drug 5-FU and hydrophobic anticancer model drug paeonolum were located in the vehicle's bond water and lipid bilayer membranes, respectively. The release behavior could be adjusted by the molar ratio of CTAB/SDBS in the vehicle solution conveniently.

**3.1.3. Gene delivery**—Silencing of gene expression by small-interfering RNA (siRNA) represents a potential strategy for cancer therapy. siRNA formulations such as microsphere encapsulation and nanoparticle complexation have been developed.<sup>[118]</sup> Although good transfection efficiencies and cellular responses are demonstrated, the transient effect limits their application. Electrospun nanofiber mediated siRNA delivery may serve as a potential alternative since the nanofiber can provide sustained long term delivery at the tumor site. In a related work, Chew *et al.* demonstrated the feasibility of loading siRNA and transfection reagent into electrospun fibers with a 28-day sustained release and 30.9% gene knockdown

efficiency.<sup>[119]</sup> Hadjiargyrou *et al.* incorporated plasmid DNA encoding small/short hairpin RNA (shRNA), against the cell cycle specific protein Cdk2, into PCL electrospun nanofibers.<sup>[42]</sup> It was found that the DNA loaded electrospun nanofiber scaffolds were capable of delivering intact and bioactive plasmid DNA for over 21 days, leading to 40% decrease in the proliferation of MCF-7 breast cancer cells.

Stem cells are traditionally used in regenerative medicine and can be manipulated to fight malignant tumors. Owing to the advances of molecular biology, human mesenchymal stem cells can be genetically engineered to secrete robust antitumor agents (e.g., tumor necrosis factor-related apoptosis-inducing ligand (TRAIL)).<sup>[120]</sup> The engineered stem cells mediated therapy shows promise for the treatment of the incurable glioblastoma. Similar to traditional stem cell therapy for regenerative medicine, after the surgical removal of glioblastoma, retention of the engineered stem cells in the surgical cavity is a great challenge. To address this problem, Hingtgen *et al.* developed TRAIL secreting stem cells cultured on electrospun PLA nanofiber implants capable of releasing the anti-tumor protein TRAIL. The results divulged an effective inhibition of regrowth of residual glioblastoma and a significantly longer median survival time in mice after implantation to the surgical cavity, in comparison to cells without releasing TRAIL cultured on nanofiber implants.<sup>[16]</sup>

### 3.2. Combinatorial/Synergistic Therapy

It is well known that cancers result from abnormal proliferation, angiogenesis, and invasion of healthy tissues. Therefore, a synergistic therapy which can simultaneously suppress proliferation, angiogenesis and invasion may be optimal for cancer therapy. To this end, Wang *et al.* demonstrated a gene/drug dual delivery system to combine RNA interference and chemotherapy for brain tumor therapy, in which anticancer drug PTX was used for blocking tumor cell proliferation, and MMP-2 RNAi plasmids, suppressing the expression of the endogenous gene MMP-2, was used for the inhibition of cancer cell invasion and angiogenesis.<sup>[43]</sup> In this study, gene/drug encapsulated PLGA fibers were electrospun from emulsion with polyethylenimine (PEI)/DNA nanoparticle suspension as the aqueous phase, and a mixture of PTX, polyethylene glycol (PEG) and PLGA solution as the organic phase, resulting in a tunable sustained release of the two agents. Most importantly, the *in vivo* study with intracranial xenograft tumor model in BALB/c nude mice indicated that the gene/drug dual delivery microfibers showed better tumor inhibition effect as compared to single drug delivery microfibers and commercial drug treatment. These studies testify the advantage of combinatorial/synergistic therapy for cancer suppression.

### 3.3. Cancer Cell Detection/Biosensing

Electrospun nanofibers have drawn wide attention for biosensor development with the aim of rapid and sensitive detection of cancer biomarkers. This can be attributed to the high surface-to-volume ratio of nanofibers and relatively defect free features even at the molecular level. Singh *et al.* developed multiwalled carbon nanotubes (MWCNT) embedded ZnO nanofiber based immunosensor for the detection of carcinoma antigen-125, which is located on the surface of ovarian cancer cells.<sup>[20]</sup> The MWCNT-ZnO electrochemical biosensor platform was prepared by calcination of MWCNT/ZnO electrospun fibers, followed by covalent conjugation of the anti-CA-125 antibody. The *in vitro* study

demonstrated an excellent sensitivity of  $90.14 \mu\text{A}/(\text{U}/\text{mL})/\text{cm}^2$  with a remarkable detection limit of  $0.00113 \text{ U}/\text{mL}$  concentration and a wide detection range of  $0.001 \text{ U}/\text{mL} - 1 \text{ kU}/\text{mL}$  (Figure 4A). In a different study, Dong *et al.* reported a microfluidic immune-biochip with femtomolar sensitivity and high selectivity for the detection of breast cancer biomarker epidermal growth factor receptor 2 (EGFR2 or ErbB2) proteins.<sup>[121]</sup> The immunoelectrode was made of porous graphene foam modified with electrospun carbon-doped titanium dioxide ( $\text{TiO}_2$ ) nanofibers. The sensor exhibited high sensitivities of  $0.585 \mu\text{A}/\mu\text{M}/\text{cm}^2$  in a wide concentration range of target ErbB2 antigen from  $1 \times 10^{-15} \text{ M}$  ( $1.0 \text{ fM}$ ) to  $0.1 \times 10^{-6} \text{ M}$  ( $0.1 \mu\text{M}$ ). The overexpression of matrix metalloproteinases, a group of enzymes responsible for degradation of extracellular matrix components, is another biomarker for cancer progression. Koh *et al.* fabricated a hydrogel-framed electrospun polystyrene/poly(styrene-alt-maleic anhydride) (PS/PSMA) nanofiber matrix integrated with a microfluidic device for the detection of matrix metalloproteinases 9, a promising target for cancer diagnosis on the basis of its massive up-regulation in malignant tissues.<sup>[122]</sup> Interestingly, the incorporation of hydrogel micropatterns into PS/PSMA electrospun matrix allowed for easy handling and insertion into the microfluidic devices. Basically, fluorescein isocyanate (FITC)-labeled MMP-9 specific peptides were covalently immobilized onto electrospun nanofiber matrix for fluorescent detection based on enzymatic cleavage strategy. A fast response time of 30 min and lower detection limit of 10 pM were achieved, which can be ascribed to the porous nature and large surface area of the nanofiber substrates (Figure 4B). In another study, Malhotra *et al.* utilized poly(3,4-ethylenedioxythiophene):poly(4-styrenesulfonate)/PVA (PEDOT:PSS/PVA) electrospun fibers for the fabrication of paper based conductive platform, and monoclonal carcinoembryonic antibodies were physically absorbed onto the PEDOT:PSS/PVA nanofibers for cancer biomarker detection.<sup>[102]</sup> This conducting paper based biosensor demonstrated an improved sensing performance with a linear detection range of  $0.2-25 \text{ ng}/\text{mL}$ , high sensitivity of  $14.2 \mu\text{A}/\text{ng mL}/\text{cm}^2$ , and shelf life of 22 days for the detection of a cancer biomarker carcinoembryonic antigen (Figure 4C). Based on the phenomenon that cancer cells consume glucose and release lactate, Thundat *et al.* deposited pH sensitive PVA/PAA electrospun nanofibers on the light addressable potentiometric sensor surface for measuring cancer cell acidification to understand metabolic activities of cancer cells and their response to chemotherapies in a noninvasive fashion (Figure 4D).<sup>[123]</sup> The electrospun nanofibers detected localized changes in pH of the media with a sensitivity response of  $74 \text{ mV}/\text{pH}$ . Oxygen is another critical component in cancer cell biology. Lannutti *et al.* developed core/shell structured fibers with PCL as shell and oxygen-sensitive probe, tris(4,7-diphenyl-1,10-phenanthroline) ruthenium(II) ( $\text{Ru}(\text{dpp})$ ) and platinum octaethylporphyrin ( $\text{PtOEP}$ ) containing polydimethylsiloxane (PDMS) as the core, for oxygen detection.<sup>[124]</sup> It was found that the sensor exhibited rapid response within 0.5 s due to the porous structure of the nanofibers and the excellent oxygen permeability of PDMS. Table 2 shows the representative electrospun nanofiber-based biosensors for cancer cell detection. These studies demonstrate that electrospun nanofibers can be combined with electrochemical sensors to develop diagnostic devices for cancer detection.



### 3.4. Drug Delivery and Cell Imaging

Introduction of distinct luminescence property into drug delivery systems renders fascinating feature of fluorescent imaging and real-time monitoring of drug delivery. The combination of drug delivery and cell imaging culminating in cancer theranostics could meet the requirement of diagnosis and therapy in cancer research.<sup>[126]</sup>

Multifunctional hollow/mesoporous nanospheres have been widely employed as carriers for drug delivery, targeted diagnosis and therapy, and fluorescent bioimaging. Although the use of nanoparticles for drug delivery and cell imaging has been demonstrated with considerable success, nanoparticles have the disadvantages of unpredictable burst release, and chemical and physical instability *in vivo*. One approach to overcome this limitation is to encapsulate multifunctional nanoparticles into electrospun nanofibers, offering a long-term release locally. Driven by this goal, magnetic Na(Y/Gd)F<sub>4</sub>:Yb<sup>3+</sup>, Er<sup>3+</sup> nanocrystals and up-conversion luminescent molecules were encapsulated into hydroxyapatite fibers through high temperature treatment of Na(Y/Gd)F<sub>4</sub>:Yb<sup>3+</sup>, Er<sup>3+</sup> nanocrystals decorated electrospun precursor fibers.<sup>[21]</sup> The porous hydroxyapatite nanofibers can be employed as a carrier for loading and delivery of drugs, protein, genes, or siRNA. In addition, the composite fibers uptaken by MC3T3-E1 cells exhibited up-conversion luminescent emission of Er<sup>3+</sup>, under 980 nm laser excitation. Further, the composite fibers could also serve as T1 MRI contrast agents due to the positive signal-enhancement ability of Gd<sup>3+</sup>. In another work, porous NaYF<sub>4</sub>:Yb<sup>3+</sup>, Er<sup>3+</sup>@SiO<sub>2</sub> nanocomposite electrospun fibers were prepared for anti-cancer drug delivery and cell imaging.<sup>[127]</sup> The DOX-loaded NaYF<sub>4</sub>:Yb<sup>3+</sup>, Er<sup>3+</sup>@SiO<sub>2</sub> nanocomposite fibers were obtained by electrospinning of precursor solution containing  $\alpha$ -NaYF<sub>4</sub>:Yb<sup>3+</sup>, Er<sup>3+</sup> nanocrystals, and annealing at 550 °C, followed by dispersion in DOX aqueous solution. The as-prepared DOX-NaYF<sub>4</sub>:Yb<sup>3+</sup>, Er<sup>3+</sup>@SiO<sub>2</sub> composite nanofibers exhibited sustained release of DOX in a pH-sensitive manner. When the nanofibers were taken up by HeLa cells through endocytosis, the released DOX induced cell death, and on the other hand, the fibers inside the cells showed near-infrared up-conversion luminescence for cell bioimaging. These results suggest that the combination of multifunctional nanoparticles and electrospun fibers has potential applications for simultaneous drug delivery and dual modal imaging.

### 3.5. Circulating Tumor Cells Separation/Capture/Isolation/Filtration

Circulating tumor cells (CTCs) are cells that shed into the vasculature or lymphatics from a primary tumor, circulated in the bloodstreams, and may provide seeds for the subsequent growth of additional tumors (metastasis) in vital distant organs.<sup>[128]</sup> The identification of CTCs is an attractive new approach in clinical cancer diagnostics,<sup>[129]</sup> while the capture of CTCs may slow down or prevent cancer metastasis. It is a great challenge to identify and capture the relatively low number of CTCs among many healthy blood cells in the body. To address this problem, electrospun nanofibers functionalized with specific biomarker molecules such as aptamers and antibodies have been employed as a substrate for cancer cell capture. Shi *et al.* immobilized HA, which targets CD44 receptors overexpressed in various carcinomas such as breast and lung tumors, onto electrospun PVA/PEI nanofibers for capturing CD44 receptor-overexpressing cancer cells.<sup>[103]</sup> The HA-modified PVA/PEI nanofibers displayed good cytocompatibility and hemocompatibility. Importantly, the

functionalized nanofibers exhibited superior capability in capturing CD44 receptor-overexpressing cancer cells (Figure 5A). In a work reported by Wu *et al.*, electrospun organic-inorganic cholesteryl-succinyl silane nanofibers were modified with membrane-bound molecules, including NBD-conjugated phospholipids and CD-20 antibodies that specifically target B lymphocytes.<sup>[130]</sup> It was found that the functionalized nanofibers exhibited a better ability to capture Granta-22 cells (Figure 5B). In another work, Zhang *et al.* first fabricated a TiO<sub>2</sub> nanofiber substrate through calcination of electrospun titanium n-butoxide (TBT)/PVP fibers.<sup>[22]</sup> Then, they introduced streptavidin (SA) onto the surface of the N-maleimidobutyryloxy succinimide ester (GMBS) coated TiO<sub>2</sub> nanofiber using N-hydroxysuccinimide (NHS)/maleimide chemistry. Finally, biotinylated epithelial cell adhesion molecule antibody (anti-EpCAM) was conjugated onto the streptavidin-coated substrates (Figure 5C). The *in vitro* results showed that the electrospun TiO<sub>2</sub> nanofiber-based cell capture device was capable of capturing cancer cells from artificial CTCs blood samples, as well as whole blood samples collected from colorectal and gastric cancer patients. These encouraging results may be attributed to the introduction of epithelial cell adhesion molecule antibody, which exhibited outstanding cell capture efficiency ranging from 40 to 70% when employed to isolate viable cancer cells from whole blood samples<sup>[131]</sup>. However, EpCAM expression on the surface of tumor cells fades away when tumor cells turn into CTCs and this marker is also expressed in mesenchymal cells, making EpCAM-based tests less accurate.<sup>[132]</sup> In addition, electrospun fiber-embedded microchip has been developed for detection, isolation, and molecular analysis of CTCs. Tseng *et al.* utilized anti-CD146 antibody (melanoma-specific capture agent) conjugated PLGA-nanofiber embedded nanovelcro chips to capture single circulating melanoma cells (Figure 5D).<sup>[133]</sup> One of the difficulties to address this problem is a shortage of broad-spectrum CTCs capture agents as most of the antibodies are only able to identify few types of cancer cells. Kang *et al.* recently found an engineered human blood opsonin protein FcMBL which could target CTCs in a broad-spectrum.<sup>[132]</sup> Although many efforts have been devoted to the detection and isolation of CTCs with improved avidity and efficiency, many challenges still exist. The current CTC tests have not been transferred to clinical trials mainly due to the lack of common biomarkers for cancers, and limited sensitivity. In the future, with the discovery of new cancer biomarkers and improvement of surface immobilization techniques, nanofiber-based devices could make a great contribution to CTCs detection and isolation.

### 3.6. Regulation of Cancer Cell Behavior

Cancer metastasis is the major cause of death worldwide.<sup>[134]</sup> During cancer metastasis, ECM remodeling occurs where the cancer cells undergo a phenotypic change that allows their migration, and invasion into the blood vessels.<sup>[135]</sup> Unfortunately, the complexity of the *in vivo* system makes it difficult to identify the ECM topographical cues that trigger cancer cell migration. Electrospinning produces randomly oriented and aligned ultrafine fibers, the microstructure and morphology of which closely resembles the cancer cell ECM. Therefore, electrospun nanofibers provide an emerging platform for the investigation of cancer cell migration in response to the surrounding ECM signaling. A limited capability in reproducing native cell motility is the major drawback of the conventional migration assays. Aligned nanofibers could offer a more physiologically relevant model to examine the migratory potential of metastatic cancer cells. Lannutti *et al.* fabricated electrospun fiber-integrated

gel-based chemotaxis system, and assessed the migratory potential of MCF-10A, MCF-7, and MDA-MB-231 cancer cells.<sup>[104]</sup> It was observed that cells traveled ~2–5 fold longer distances cultured on aligned fibers. And more highly metastatic MDA-MB-231 cells migrated further and at greater velocities as compared to the less metastatic MCF-7 cells. Viapiano *et al.* utilized highly aligned PCL nanofibers to mimic the neural topography, and examined the motility, gene expression, and sensitivity to migration inhibitors of glioma cells cultured on the fibers.<sup>[136]</sup> The glioma cells on the aligned nanofibers could recapitulate an elongated morphology of migrating cells in white matter tissue. Also, the activation of the transcription factor STAT3, a central regulator of tumor progression and metastasis in solid cancers, was demonstrated. Wang *et al.* evaluated the impact of fiber orders on breast cancer cell response.<sup>[106]</sup> The uniaxially aligned electrospun nanofibers promoted breast cancer cell alignment and induced epithelium to mesenchymal transformation (EMT)-like phenotype formation, suggesting fiber alignment can make cancer cells gain migratory and invasive properties.

Other than the studies on the cell migration, studies also examined the effect of electrospun nanofiber substrate on chemoresistance, which is a major cause for the failure of current chemotherapy. Kmiec *et al.* used PCL/Chitosan nanofiber as the culture substrate to explore the behavior of breast cancer stem-like cells (BCSCs), which are highly resistant to chemotherapy.<sup>[137]</sup> It was found that BCSCs cultured on PCL/Chitosan nanofibers showed an increase in mammary stem cell markers and in sphere-forming ability as compared to those cultured on polystyrene culture dishes. In addition, the results suggested that BCSCs cultured on nanofibers may inhibit their differentiation and increase their resistance to docetaxel and doxorubicin.

By making use of the nanotopographic cues rendered by aligned nanofibers, a new anticancer therapeutic approach could be developed. Bellamkonda *et al.* designed a ‘tumor guide’ device composed of aligned PCL nanofibers which structurally mimics the white matter tracts and blood vessels to guide the invasive tumor cell migration away from the primary tumor site to an extracortical location, then induce apoptosis (Figure 6A).<sup>[23]</sup> The *in vitro* results showed that the glioblastoma U87MG-eGFP cells elongated on the aligned fibers, as compared to the polygonal shape on the smooth film, and the cells migrated 4 to 4.5 mm on the aligned nanofiber, as compared to that of 1.5 mm on the smooth films over 10 days (Figure 6B). A significant number of glioblastoma cells migrated along the aligned nanofibers, and underwent apoptosis in the cyclopamine-releasing collagen hydrogel on the cortical surface (Figure 6C), resulting in a pronounced reduction in the total tumor volume compared with those without implant and the smooth film implant. This approach provides a new therapeutic strategy of relocating and inhibiting the growth of primary tumors.

Spurred by the recent progress in 3D scaffold fabrication and oncology, a precise study of the factors regulating cancer cell behavior in 3D matrices has become possible. Compared with hydrogels, the fibrous scaffolds provide a high surface area and porosity for carrying physiological molecules with better mimicry of cancer cell ECM. However, an optimal scaffold or 3D model has not been standardized yet. One another interesting extension in future work would be to introduce stimuli-responsive systems to achieve on-demand local

delivery of chemo-therapeutic agents after relocation of cancer cells from the primary tumor site.

### 3.7. Engineering 3D Cancer Model *in vitro*

*In vitro* cancer model provides a powerful tool for cancer research, including identification of carcinogens, development of cancer therapies, drug screening, and exploration of molecular mechanisms of tumor growth and metastasis.<sup>[11]</sup> A body of valuable information has been obtained from conventional *in vitro* 2D studies, in which cells are cultured on flat and hard plastic dishes or flasks. In recent years, there is an increasing evidence on the inability of 2D systems to recapitulate the 3D microenvironment that cancer cells live in, due to the lack of complex and dynamic cell-cell communications and cell-matrix interactions that occur during cancer metastasis.<sup>[138]</sup> To overcome these deficiencies, a number of 3D tumor models have been proposed, in the form of microfluidic devices<sup>[139]</sup>, natural and synthetic polymer scaffold or hydrogel<sup>[140]</sup>, and spheroids<sup>[141]</sup>. Among them, electrospun nanofiber scaffolds provide an alternative artificial 3D culture matrix due to their biomimicry of the architecture and composition of ECM<sup>[142]</sup>, and high versatility in biochemical stimuli, including growth factors, adhesion molecules, and drugs<sup>[12,143]</sup>. Cells cultured on the scaffolds respond to the biochemical stimuli through specific interactions between cell surface receptors and the immobilized ligands. Choi *et al.* used 3D electrospun scaffolds composed of poly(3-hydroxybutyrate-co-3-hydroxyvalerate) and collagen peptide as a gastric cancer model for chemosensitivity test.<sup>[19]</sup> A higher concentration of anti-cancer drugs was needed in 3D culture to achieve comparable cytotoxic effects, indicating an increased drug resistance in 3D culture compared with 2D culture. During cancer cell metastasis to bone, such as prostate and breast cancer types, bone matrix proteins confer enhanced cancer cell adhesion, migration and invasion.<sup>[144]</sup> For example, Hartman *et al.* employed perlecan domain IV (PInDIV) peptide conjugated 3D PCL/gelatin electrospun nanofiber scaffolds as a prostate cancer model for pharmacokinetic study.<sup>[12]</sup> It was found that PInDIV peptide functionalized scaffold supported proliferation, survival and migration of C4-2B cancer cells. In another work, Mikos *et al.* developed an *ex vivo* ewing sarcoma model based on the use of 3D electrospun PCL fiber scaffolds, resulting in a more physiologically relevant ES cell phenotype compared to conventional monolayer cultures.<sup>[145]</sup> The 3D ewing sarcoma model also showed a significant upregulation of the insulin-like growth factor pathway, which is a receptor normally expressed in ewing sarcoma and an important target for drug development.

Although these 3D models are promising in bridging the gap between *in vitro* and *in vivo* testing in terms of cell proliferation<sup>[146]</sup>, gene expression<sup>[146]</sup>, and drug resistance<sup>[147]</sup>, they fail to mimic some specific activities occurring in the tumor microenvironment including heterotypic cell-cell signaling, cell motility, tumor angiogenesis, tumor cell metabolism, and biomechanical stimulation.<sup>[101]</sup> Among them, biomechanical stimulation plays a crucial role in tumor progression and metastasis<sup>[148]</sup>, which has been added to the 3D system as a new feature to mimic *in vivo* ewing sarcoma biology and drug sensitivity. Mikos *et al.* developed an *ex vivo* ewing sarcoma (a translocation-positive bone tumor) model composed of 3D electrospun PCL nanofiber scaffolds and a flow perfusion bioreactor which provides mechanical stimulation in the form of flow-derived shear stress.<sup>[101]</sup> The convective flow

promoted nutrient delivery, resulting in more uniform cell distribution and higher proliferation (Figure 7). Moreover, the flow-derived shear stress demonstrated an enhanced insulin-like growth factor-1 (IGF1) production and significant upregulation of the IGF1 receptor (IGF-1R) expression, one of the most promising targets in preclinical and early-phase drug development. Additionally, flow perfusion enhanced the drug sensitivity of IGF-1R inhibitor dalotuzumab (MK-0646) on ewing sarcoma cells in a dose dependent manner.

Cellular infiltration throughout 3D nanofiber scaffolds is the key of an engineered cancer model. Although larger-sized fibers and mechanical stimulation have been employed to enhance cell penetration into 3D scaffolds to some degree, there is still room for improvement of cellular infiltration by optimizing the fabrication of 3D fiber scaffolds. For example, nanofiber aerogels with interconnected pores have been generated by freeze-drying of short nanofiber solutions.<sup>[109]</sup> Such aerogels could be used as scaffolds for engineering 3D *in vitro* cancer models as cells can be easily cultured throughout the whole material. In addition, highly porous 3D electrospun nanofiber scaffolds with hierarchical structure and maintenance of aligned nanotopographic cues could be used to engineer 3D cancer models for studying cancer metastasis. Combining 3D nanofiber scaffolds with hydrogels to form a hybrid system may better recapitulate the microenvironment of cancer cells.

Despite the considerable success in establishing 3D cancer models, huge challenges still exist and significant improvements need to be made in the optimization and standardization of such models. Firstly, matrix-assisted assembly of 3D cancer models have not been widely employed for high-throughput drug screening due to batch to batch variability and lack of scale-up capability. Secondly, although the current 3D cancer models partially represent the structure and morphology, they cannot recapitulate the features of native tumor microenvironment, especially the physiological complexity and heterogeneous feature. In the future, the combination of 3D printing technology and electrospinning may be the next further step towards more sophisticated 3D cancer models. The optimal 3D cancer models would promote the translation of new therapeutics to clinical trials.

### 3.8. Engineering Bone Tissue for Cancer Metastasis Study

Metastasis is responsible for more than 90% of cancer-related deaths.<sup>[149]</sup> Bone metastases occur in up to 70 % of patients with advanced breast or prostate cancer, and in approximately 40% of patients with carcinoma of the lung, kidney, or thyroid cancer.<sup>[150]</sup> However, detailed mechanisms of cancer bone metastasis remain poorly understood.<sup>[151]</sup> Previous studies showed that prostate and breast cancers tend to migrate into the adjacent bone<sup>[152]</sup>, suggesting bone matrix may contribute to the increased cancer cell growth, adhesion, migration and invasion<sup>[153]</sup>. Thus, engineered bone tissues provide a promising *in vitro* model for cancer metastasis study. The design of electrospun fiber scaffolds for study of cancer metastasis to bone is inspired by the need to mimic the bone marrow environment and functionally reproduce their biological features. Holzapfel *et al.* developed tubular PCL scaffolds by melt-electrospinning with a combination of human mesenchymal cells and rhBMP-7 for a humanized bone organ. The composite scaffold caused homing and proliferation of human prostate cancer cells, and macro-metastase development (Figure 8).

[154] In a different study, Hartman *et al.* reported electrospun PCL scaffolds with tailored physical properties and biological functionalization with a bioactive peptide derived from domain IV of perlecan heparin sulfate proteoglycan to recreate the bone marrow microenvironment. The peptide enhanced adhesion, spreading and infiltration of the metastatic prostate cancer cells on the scaffolds.<sup>[24]</sup> Future work may consider incorporating hydroxyapatite through surface coating or physically blending to electrospun scaffolds to partially mimic the composition of mineralized bone.

## 4. Conclusions and Future Directions

In summary, we have provided an overview of the recent progress of electrospun nanofibers in cancer research. This progress report highlighted the applications of electrospun nanofibers in drug/gene delivery, cancer cell detection/capture, cancer cell imaging, regulation of cancer cell behavior, construction of *in vitro* 3D cancer model, and engineering bone microenvironment for cancer metastasis.

Previous studies investigated the use of electrospun nanofibers mainly for local drug delivery. Due to their biomimicry, electrospun nanofibers, in particular 3D nanofiber scaffolds, have been widely examined as scaffolds for tissue regeneration.<sup>[155]</sup> Future studies may consider combining these two concepts to develop nanofiber drug delivery devices which can topically release drugs in a sustained manner and simultaneously promote tissue regeneration to fill the resected void space.

Although there is some progress on the fabrication of 3D electrospun nanofiber scaffolds, engineering 3D *in vitro* cancer models is still a challenge to closely mimic the physiology of solid tumors due to genotypic and phenotypic tumor heterogeneity. The current research efforts of 3D printing mainly focus on tissue engineering applications and may also be applied for the development of 3D *in vitro* cancer models.<sup>[156]</sup> Intriguingly, electrospinning has been combined with 3D printing to fabricate 3D hierarchical scaffolds.<sup>[157]</sup> The future direction may be to consider exploring a combination of electrospinning and 3D printing towards the development of an elaborated 3D *in vitro* cancer model.

Current strategies for cancer therapy mainly include surgery, radiotherapy, chemotherapy, immunotherapy and their combinations. Approximately 50% of the cancer patients receive radiotherapy, including external beam, localized internal irradiation, and combination of chemotherapy.<sup>[158]</sup> The administration of radiosensitizing drugs by the drug delivery system can enhance the antitumor radiation efficacy.<sup>[159]</sup> It is expected that the addition of radiosensitization to nanofiber-based drug delivery systems can contribute to their therapeutic efficacy.

As breast, prostate, and lung cancers often metastasize to bone, future studies may consider developing an engineered bone niche based on electrospun nanofibers which can attract/home metastatic cancer cells to the niche after subcutaneous implantation for early cancer metastasis detection and subsequently release anticancer drugs to induce apoptosis of recruited cancer cells for therapy.<sup>[160]</sup>



Preclinical studies for testing electrospun nanofiber drug delivery devices mostly comprise xenografts or orthotopic cancer models in rodents. Spontaneous and transgenic large animal tumor models like engineered swine cancer models may be more valuable for preclinical studies in terms of clinical relevance and their safety and toxicity testing.<sup>[161]</sup>

Despite great progress and promise, most studies are still limited to the preclinical studies. There is an imperative need to develop a viable strategy to rapidly translate the use of electrospun nanofibers from bench to clinical trials for diagnosis and treatment of devastating cancers. For example, pancreatic ductal adenocarcinoma is the fourth most common cause of death from cancer in the USA, having a five-year survival rate less than 5%.<sup>[162]</sup> At the time of diagnosis, around 20% of patients are presented with resectable cancer.<sup>[163]</sup> But even in patients with R0 resected tumors, five-year survival rate is less than 20% with a median survival time between 12 and 20 months. Chemotherapy is often used after resection of the cancer to prevent recurrent growth and metastasis of remaining malignant cells.<sup>[164]</sup> Unfortunately, the efficacy of chemotherapy for pancreatic cancer is impaired by a unique desmoplastic response.<sup>[165]</sup> An electrospun nanofiber local drug delivery device capable of overcoming this barrier could provide substantial benefit for patients with resectable pancreatic cancer and locally advanced pancreatic cancer.

## Acknowledgments

This work was supported partially from startup funds from University of Nebraska Medical Center (UNMC), National Institute of General Medical Science (NIGMS) grant 2P20 GM103480-06, National Institute of General Medical Science (NIGMS) of the National Institutes of Health under Award Number R01GM123081, and UNMC Regenerative Medicine Program pilot project grant number 37-1209-2004-007 and Otis Glebe Medical Research Foundation.

## References

1. Siegel RL, Miller KD, Jemal A. CA Cancer J. Clin. 2016; 66:7. [PubMed: 26742998]
2. Thoma CR, Zimmermann M, Agarkova I, Kelm JM, Krek W. Adv. Drug Deliv. Rev. 2014; 69:29. [PubMed: 24636868]
3. a) Kievit FM, Florczyk SJ, Leung MC, Wang K, Wu JD, Silber JR, Ellenbogen RG, Lee JSH, Zhang M. Biomaterials. 2014; 35:9137. [PubMed: 25109438] b) Kievit FM, Florczyk SJ, Leung MC, Veiseh O, Park JO, Disis ML, Zhang M. Biomaterials. 2010; 31:5903. [PubMed: 20417555]
4. Ranganath SH, Wang C-H. Biomaterials. 2008; 29:2996. [PubMed: 18423584]
5. Hutmacher DW. Nat. Mater. 2010; 9:90. [PubMed: 20094076]
6. Soman P, Kelber JA, Lee JW, Wright TN, Vecchio KS, Klemke RL, Chen S. Biomaterials. 2012; 33:7064. [PubMed: 22809641]
7. Branco MC, Sigano DM, Schneider JP. Curr. Opin. Chem. Biol. 2011; 15:427. [PubMed: 21507707]
8. Kievit FM, Wang FY, Fang C, Mok H, Wang K, Silber JR, Ellenbogen RG, Zhang M. J. Control. Release. 2011; 152:76. [PubMed: 21277920]
9. Hinderer S, Layland SL, Schenke-Layland K. Adv. Drug Deliv. Rev. 2016; 97:260. [PubMed: 26658243]
10. Wang R, Xu J, Juliette L, Castilleja A, Love J, Sung SY, Zhau HE, Goodwin TJ, Chung LWK. Semin. Cancer Biol. 2005; 15:353. [PubMed: 15982899]
11. Xu X, Farach-Carson MC, Jia X. Biotechnol. Adv. 2014; 32:1256. [PubMed: 25116894]
12. Hartman O, Zhang C, Adams EL, Farach-Carson MC, Petrelli NJ, Chase BD, Rabolt JF. Biomaterials. 2010; 31:5700. [PubMed: 20417554]
13. Brigger I, Dubernet C, Couvreur P. Adv. Drug Deliv. Rev. 2002; 54:631. [PubMed: 12204596]

14. Ta HT, Dass CR, Dunstan DE. J. Control. Release. 2008; 126:205. [PubMed: 18258328]
15. Ramachandran R, Junnuthula VR, Gowd GS, Ashokan A, Thomas J, Peethambaran R, Thomas A, Unni AK, Panikar D, Nair SV, Koyakutty M. Sci. Rep. 2017; 7:43271. [PubMed: 28262735]
16. Bagó JR, Pegna GJ, Okolie O, Mohiti-Asli M, Lobo EG, Hingtgen SD. Biomaterials. 2016; 90:116. [PubMed: 27016620]
17. Wei J, Luo X, Chen M, Lu J, Li X. Acta Biomater. 2015; 23:189. [PubMed: 26013039]
18. Kim YJ, Ebara M, Aoyagi T. Adv. Funct. Mater. 2013; 23:5753.
19. Kim Y-J, Bae H-I, Kwon OK, Choi M-S. Int. J. Biol. Macromol. 2009; 45:65. [PubMed: 19375451]
20. Paul KB, Singh V, Vanjari SRK, Singh SG. Biosens. Bioelectron. 2017; 88:144. [PubMed: 27520500]
21. Liu M, Liu H, Sun S, Li X, Zhou Y, Hou Z, Lin J. Langmuir. 2014; 30:1176. [PubMed: 24432899]
22. Zhang N, Deng Y, Tai Q, Cheng B, Zhao L, Shen Q, He R, Hong L, Liu W, Guo S, Liu K, Tseng HR, Xiong B, Zhao XZ. Adv. Mater. 2012; 24:2756. [PubMed: 22528884]
23. Jain A, Betancur M, Patel GD, Valmikinathan CM, Mukhatyar VJ, Vakharia A, Pai SB, Brahma B, MacDonald TJ, Bellamkonda RV. Nat. Mater. 2014; 13:308. [PubMed: 24531400]
24. Hartman O, Zhang C, Adams EL, Farach-Carson MC, Petrelli NJ, Chase BD, Rabolt JF. Biomaterials. 2010; 31:5700. [PubMed: 20417554]
25. Kenawy E-R, Bowlin GL, Mansfield K, Layman J, Simpson DG, Sanders EH, Wnek GE. J. Control. Release. 2002; 81:57. [PubMed: 11992678]
26. Pillay V, Dott C, Choonara YE, Tyagi C, Tomar L, Kumar P, du Toit LC, Ndesendo VMK. J. Nanomater. 2013; 2013
27. Yohe ST, Herrera VLM, Colson YL, Grinstaff MW. J. Control. Release. 2012; 162:92. [PubMed: 22684120]
28. a) Zong S, Wang X, Yang Y, Wu W, Li H, Ma Y, Lin W, Sun T, Huang Y, Xie Z, Yue Y, Liu S, Jing X. Eur. J. Pharm. Biopharm. 2015; 93:127. [PubMed: 25843238] b) Kaplan JA, Liu R, Freedman JD, Padera R, Schwartz J, Colson YL, Grinstaff MW. Biomaterials. 2016; 76:273. [PubMed: 26547283]
29. a) Toshkova R, Manolova N, Gardeva E, Ignatova M, Yossifova L, Rashkov I, Alexandrov M. Int. J. Pharm. 2010; 400:221. [PubMed: 20816737] b) Zheng F, Wang S, Shen M, Zhu M, Shi X. Polym. Chem. 2013; 4:933.c) Qiu K, He C, Feng W, Wang W, Zhou X, Yin Z, Chen L, Wang H, Mo X. J. Mater. Chem. B. 2013; 1:4601.d) Liu S, Zhou G, Liu D, Xie Z, Huang Y, Wang X, Wu W, Jing X. J. Mater. Chem. B. 2013; 1:101.e) Zhao X, Yuan Z, Yildirim L, Zhao J, Lin ZY, Cao Z, Pan G, Cui W. Small. 2015; 11:4284. [PubMed: 26034038] f) Jiang J, Xie J, Ma B, Bartlett DE, Xu A, Wang CH. Acta Biomater. 2014; 10:1324. [PubMed: 24287161] g) Kim Y-J, Ebara M, Aoyagi T. Adv. Funct. Mater. 2013; 23:5753.h) Yang G, Wang J, Wang Y, Li L, Guo X, Zhou S. ACS Nano. 2015; 9:1161. [PubMed: 25602381]
30. Wei J, Hu J, Li M, Chen Y, Chen Y. RCS Adv. 2014; 4:28011.
31. a) Xie J, Wang CH. Pharm. Res. 2006; 23:1817. [PubMed: 16841195] b) Ma G, Liu Y, Peng C, Fang D, He B, Nie J. Carbohydr. Polym. 2011; 86:505.
32. Xu X, Chen X, Wang Z, Jing X. Eur. J. Pharm. Biopharm. 2009; 72:18. [PubMed: 19027067]
33. Yoo JJ, Kim C, Chung CW, Jeong YI, Kang DH. Int. J. Nanomedicine. 2012; 7:1997. [PubMed: 22619537]
34. Luo X, Xie C, Wang H, Liu C, Yan S, Li X. Int. J. Pharm. 2012; 425:19. [PubMed: 22265915]
35. Luo X, Zhang H, Chen M, Wei J, Zhang Y, Li X. Int. J. Pharm. 2014; 475:438. [PubMed: 25218185]
36. Chen P, Wu QS, Ding YP, Chu M, Huang ZM, Hu W. Eur. J. Pharm. Biopharm. 2010; 76:413. [PubMed: 20854905]
37. Xu X, Chen X, Xu X, Lu T, Wang X, Yang L, Jing X. J. Control. Release. 2006; 114:307. [PubMed: 16891029]
38. Shao S, Li L, Yang G, Li J, Luo C, Gong T, Zhou S. Int. J. Pharm. 2011; 421:310. [PubMed: 21983092]

39. a) Guo G, Fu S, Zhou L, Liang H, Fan M, Luo F, Qian Z, Wei Y. *Nanoscale*. 2011; 3:3825. [PubMed: 21847493] b) Sampath M, Lakra R, Korrapati P, Sengottuvelan B. *Colloids Surf., B*. 2014; 117:128.
40. Song M, Guo D, Pan C, Jiang H, Chen C, Zhang R, Gu Z, Wang X. *Nanotechnology*. 2008; 19:165102. [PubMed: 21825633]
41. Lv G, He F, Wang X, Gao F, Zhang G, Wang T, Jiang H, Wu C, Guo D, Li X, Chen B, Gu Z. *Langmuir*. 2008; 24:2151. [PubMed: 18193905]
42. Achille C, Sundaresh S, Chu B, Hadjiargyrou M. *PLoS One*. 2012; 7:e52356. [PubMed: 23285007]
43. Lei C, Cui Y, Zheng L, Chow PK, Wang CH. *Biomaterials*. 2013; 34:7483. [PubMed: 23820014]
44. Okada T, Niiyama E, Uto K, Aoyagi T, Ebara M. *Materials*. 2015; 9:12.
45. Lin TC, Lin FH, Lin JC. *Acta Biomater*. 2012; 8:2704. [PubMed: 22484694]
46. Zeng J, Yang L, Liang Q, Zhang X, Guan H, Xu X, Chen X, Jing X. *J. Control. Release*. 2005; 105:43. [PubMed: 15908033]
47. Sultanova Z, Kaleli G, Kabay G, Mutlu M. *Int. J. Pharm*. 2016; 505:133. [PubMed: 27012983]
48. Kim K, Luu YK, Chang C, Fang D, Hsiao BS, Chu B, Hadjiargyrou M. *J. Control. Release*. 2004; 98:47. [PubMed: 15245888]
49. Qi H, Hu P, Xu J, Wang A. *Biomacromolecules*. 2006; 7:2327. [PubMed: 16903678]
50. Han D, Steckl AJ. *ACS Appl. Mater. Interfaces*. 2013; 5:8241. [PubMed: 23924226]
51. Song B, Wu C, Chang J. *Acta Biomater*. 2012; 8:1901. [PubMed: 22326789]
52. Xie J, MacEwan MR, Li X, Sakiyama-Elbert SE, Xia Y. *ACS Nano*. 2009; 3:1151. [PubMed: 19397333]
53. Xie J, Liu W, MacEwan MR, Bridgman PC, Xia Y. *ACS Nano*. 2014; 8:1878. [PubMed: 24444076]
54. Xie J, MacEwan MR, Willerth SM, Li X, Moran DW, Sakiyama-Elbert SE, Xia Y. *Adv. Funct. Mater*. 2009; 19:2312. [PubMed: 19830261]
55. a) Li X, Xie J, Lipner J, Yuan X, Thomopoulos S, Xia Y. *Nano Lett*. 2009; 9:2763. [PubMed: 19537737] b) Xie J, Zhong S, Ma B, Shuler FD, Lim CT. *Acta Biomater*. 2013; 9:5698. [PubMed: 23131385]
56. Peng Q, Sun X-Y, Spagnola JC, Hyde GK, Spontak RJ, Parsons GN. *Nano Lett*. 2007; 7:719. [PubMed: 17279801]
57. Li X, Xie J, Yuan X, Xia Y. *Langmuir*. 2008; 24:14145. [PubMed: 19053657]
58. Ahmed I, Liu HY, Mamiya PC, Ponery AS, Babu AN, Weik T, Schindler M, Meiners S. *J Biomed Mater Res A*. 2006; 76:851. [PubMed: 16345089]
59. Yoo HS, Kim TG, Park TG. *Adv. Drug Deliv. Rev*. 2009; 61:1033. [PubMed: 19643152]
60. Kurooka M, Kaneda Y. *Cancer Res*. 2007; 67:227. [PubMed: 17210703]
61. Yang GZ, Li JJ, Yu DG, He MF, Yang JH, Williams GR. *Acta Biomater*. 2017; 53:233. [PubMed: 28137657]
62. Labbaf S, Ghanbar H, Stride E, Edirisinghe M. *Macromol. Rapid Commun*. 2014; 35:618. [PubMed: 24510905]
63. Huang X, Brazel CS. *J. Control. Release*. 2001; 73:121. [PubMed: 11516493]
64. Li X, Su Y, Liu S, Tan L, Mo X, Ramakrishna S. *Colloids Surf B Biointerfaces*. 2010; 75:418. [PubMed: 19836931]
65. Jiang H, Wang L, Zhu K. *J. Control. Release*. 2014; 193:296. [PubMed: 24780265]
66. Zhang YZ, Wang X, Feng Y, Li J, Lim CT, Ramakrishna S. *Biomacromolecules*. 2006; 7:1049. [PubMed: 16602720]
67. Su Y, Su Q, Liu W, Lim M, Venugopal JR, Mo X, Ramakrishna S, Al-Deyab SS, El-Newehy M. *Acta Biomater*. 2012; 8:763. [PubMed: 22100346]
68. Liu W, Ni C, Chase DB, Rabolt JF. *ACS Macro Lett*. 2013; 2:466.
69. Falde EJ, Freedman JD, Herrera VLM, Yohe ST, Colson YL, Grinstaff MW. *J. Control. Release*. 2015; 214:23. [PubMed: 26160309]

70. Liu S, Wang X, Zhang Z, Zhang Y, Zhou G, Huang Y, Xie Z, Jing X. *Nanomedicine NBM*. 2015; 11:1047.
71. Okuda T, Tominaga K, Kidoaki S. *J. Control. Release*. 2010; 143:258. [PubMed: 20074599]
72. Zhang Z, Liu S, Qi Y, Zhou D, Xie Z, Jing X, Chen X, Huang Y. *J. Control. Release*. 2016; 235:125. [PubMed: 27221069]
73. Hu X, Liu S, Zhou G, Huang Y, Xie Z, Jing X. *J. Control. Release*. 2014; 185:12. [PubMed: 24768792]
74. Yohe ST, Colson YL, Grinstaff MW. *J. Am. Chem. Soc.* 2012; 134:2016. [PubMed: 22279966]
75. Ji W, Yang F, van den Beucken JJ, Bian Z, Fan M, Chen Z, Jansen JA. *Acta Biomater.* 2010; 6:4199. [PubMed: 20594971]
76. Han D, Yu X, Chai Q, Ayres N, Steckl AJ. *ACS Appl. Mater. Interfaces*. 2017; 9:11858. [PubMed: 28263054]
77. Mura S, Nicolas J, Couvreur P. *Nat. Mater.* 2013; 12:991. [PubMed: 24150417]
78. Landon CD, Park JY, Needham D, Dewhirst MW. *The open nanomedicine journal*. 2011; 3:38. [PubMed: 23807899]
79. Yohe ST, Kopechek JA, Porter TM, Colson YL, Grinstaff MW. *Adv Healthc Mater.* 2013; 2:1204. [PubMed: 23592698]
80. Yun J, Im JS, Lee Y-S, Kim H-I. *Eur. Polym. J.* 2011; 47:1893.
81. Verreck G, Chun I, Rosenblatt J, Peeters J, Dijk AV, Mensch J, Noppe M, Brewster ME. *J. Control. Release*. 2003; 92:349. [PubMed: 14568415]
82. Zeng J, Xu X, Chen X, Liang Q, Bian X, Yang L, Jing X. *J. Control. Release*. 2003; 92:227. [PubMed: 14568403]
83. Xue J, He M, Liu H, Niu Y, Crawford A, Coates PD, Chen D, Shi R, Zhang L. *Biomaterials*. 2014; 35:9395. [PubMed: 25134855]
84. Natu MV, de Sousa HC, Gil MH. *Int. J. Pharm.* 2010; 397:50. [PubMed: 20599485]
85. Zong X, Kim K, Fang D, Ran S, Hsiao BS, Chu B. *Polymer*. 2002; 43:4403.
86. Thakur RA, Florek CA, Kohn J, Michniak BB. *Int. J. Pharm.* 2008; 364:87. [PubMed: 18771719]
87. Cui W, Li X, Zhu X, Yu G, Zhou S, Weng J. *Biomacromolecules*. 2006; 7:1623. [PubMed: 16677047]
88. Yu DG, Li XY, Wang X, Yang JH, Bligh SW, Williams GR. *ACS Appl. Mater. Interfaces*. 2015; 7:18891. [PubMed: 26244640]
89. Viry L, Moulton SE, Romeo T, Suhr C, Mawad D, Cook M, Wallace GG. *J. Mater. Chem.* 2012; 22:11347.
90. Ritger PL, Peppas NA. *J. Control. Release*. 1987; 5:23.
91. a) Srikar R, Yarin AL, Megaridis CM, Bazilevsky AV, Kelley E. *Langmuir*. 2008; 24:965. [PubMed: 18076196] b) Khansari S, Duzyer S, Sinha-Ray S, Hockenberger A, Yarin AL, Pourdeyhimi B. *Mol. Pharm.* 2013; 10:4509. [PubMed: 24191694]
92. Zupancic S, Sinha-Ray S, Sinha-Ray S, Kristl J, Yarin AL. *Mol. Pharm.* 2016; 13:1393. [PubMed: 26950163]
93. Nakielski, TKP., Kowaleski, TA. *Proceeding of the COMSOL Conference*. Rotterdam: 2013 Oct 23–25.
94. Nakielski P, Kowalczyk T, Zembrzycki K, Kowalewski TA. *J. Biomed. Mater. Res. B Appl. Biomater.* 2015; 103:282. [PubMed: 24819674]
95. Dias JR, Granja PL, Bártolo PJ. *Prog. Mater. Sci.* 2016; 84:314.
96. Katta P, Alessandro M, Ramsier RD, Chase GG. *Nano Lett.* 2004; 4:2215.
97. Li D, Wang Y, Xia Y. *Adv. Mater.* 2004; 16:361.
98. Li X, Li Z, Wang L, Ma G, Meng F, Pritchard RH, Gill EL, Liu Y, Huang YY. *ACS Appl. Mater. Interfaces*. 2016; 8:32120. [PubMed: 27807979]
99. Ma B, Xie J, Jiang J, Wu J. *Biomaterials*. 2014; 35:630. [PubMed: 24144904]
100. Xie J, MacEwan MR, Ray WZ, Liu W, Siewe DY, Xia Y. *ACS Nano*. 2010; 4:5027. [PubMed: 20695478]

101. Santoro M, Lamhamedi-Cherradi S-E, Menegaz BA, Ludwig JA, Mikos AG. *Proc. Natl. Acad. Sci. USA.* 2015; 112:10304. [PubMed: 26240353]
102. Kumar S, Rai P, Sharma JG, Sharma A, Malhotra BD. *Adv. Mater. Technol.* 2016;1.
103. Zhao Y, Fan Z, Shen M, Shi X. *Adv. Mater. Interfaces.* 2015; 2:1500256.
104. Nelson MT, Short A, Cole SL, Gross AC, Winter J, Eubank TD, Lannutti JJ. *BMC cancer.* 2014; 14:825. [PubMed: 25385001]
105. Agudelo-Garcia PA, De Jesus JK, Williams SP, Nowicki MO, Chiocca EA, Liyanarachchi S, Li P-K, Lannutti JJ, Johnson JK, Lawler SE. *Neoplasia.* 2011; 13:831IN15. [PubMed: 21969816]
106. Saha S, Duan X, Wu L, Lo P-K, Chen H, Wang Q. *Langmuir.* 2011; 28:2028. [PubMed: 22182057]
107. Rnjak-Kovacina J, Weiss AS. *Tissue Eng., Part B.* 2011; 17:365.
108. a) Baker BM, Gee AO, Metter RB, Nathan AS, Marklein RA, Burdick JA, Mauck RL. *Biomaterials.* 2008; 29:2348. [PubMed: 18313138] b) Bonvallet PP, Schultz MJ, Mitchell EH, Bain JL, Culpepper BK, Thomas SJ, Bellis SL. *PloS one.* 2015; 10:e0122359. [PubMed: 25793720]
109. Si Y, Yu J, Tang X, Ge J, Ding B. *Nat. Commun.* 2014; 5:5802. [PubMed: 25512095]
110. Chen W, Ma J, Zhu L, Morsi Y, Hany EIH, Al-Deyab SS, Mo X. *Colloids Surf., B.* 2016; 142:165.
111. Sheikh FA, Ju HW, Lee JM, Moon BM, Park HJ, Lee OJ, Kim J-H, Kim D-K, Park CH. *Nanomedicine NBM.* 2015; 11:681.
112. Jiang J, Carlson MA, Teusink MJ, Wang H, MacEwan MR, Xie J. *ACS Biomater. Sci. Eng.* 2015; 1:991.
113. Jiang J, Li Z, Wang H, Wang Y, Carlson MA, Teusink MJ, MacEwan MR, Gu L, Xie J. *Adv. Healthcare Mater.* 2016; 5:2993.
114. Xie J, Ma B, Michael PL. *Adv. Healthcare Mater.* 2012; 1:674.
115. Park SH, Kim TG, Kim HC, Yang D-Y, Park TG. *Acta Biomater.* 2008; 4:1198. [PubMed: 18458008]
116. Jain V, Jain S, Mahajan SC. *Curr. Drug Delivery.* 2015; 12:177.
117. Li W, Luo T, Yang Y, Tan X, Liu L. *Langmuir.* 2015; 31:5141. [PubMed: 25897828]
118. a) Shimanovich U, Tkacz ID, Eliaz D, Cavaco-Paulo A, Michaeli S, Gedanken A. *Adv. Funct. Mater.* 2011; 21:3659. b) Trabulo S, Resina S, Simoes S, Lebleu B, Pedroso de Lima MC. *J. Control. Release.* 2010; 145:149. [PubMed: 20362021]
119. Rujitanaroj PO, Wang YC, Wang J, Chew SY. *Biomaterials.* 2011; 32:5915. [PubMed: 21596430]
120. Aboody KS, Najbauer J, Danks MK. *Gene. Ther.* 2008; 15:739. [PubMed: 18369324]
121. Ali MA, Mondal K, Jiao Y, Oren S, Xu Z, Sharma A, Dong L. *ACS Appl. Mater. Interfaces.* 2016; 8:20570. [PubMed: 27442623]
122. Han SW, Koh W-G. *Anal. Chem.* 2016; 88:6247. [PubMed: 27214657]
123. Shaibani PM, Etayash H, Naicker S, Kaur K, Thundat T. *ACS Sens.* 2017; 2:151. [PubMed: 28722424]
124. Xue R, Behera P, Xu J, Viapiano MS, Lannutti JJ. *Sensors and actuators. B, Chemical.* 2014; 192:697.
125. Ali MA, Mondal K, Singh C, Malhotra BD, Sharma A. *Nanoscale.* 2015; 7:7234. [PubMed: 25811908]
126. Huang P, Li Z, Lin J, Yang D, Gao G, Xu C, Bao L, Zhang C, Wang K, Song H, Hu H, Cui D. *Biomaterials.* 2011; 32:3447. [PubMed: 21303717]
127. Hou Z, Li C, Ma Pa, Cheng Z, Li X, Zhang X, Dai Y, Yang D, Lian H, Lin J. *Adv. Funct. Mater.* 2012; 22:2713.
128. Plaks V, Koopman CD, Werb Z. *Science.* 2013; 341:1186. [PubMed: 24031008]
129. Geiger TR, Peeper DS. *Biochim. Biophys. Acta.* 2009; 1796:293. [PubMed: 19683560]
130. Zha Z, Jiang L, Dai Z, Wu X. *Appl. Phys. Lett.* 2012; 101:193701. [PubMed: 23213266]
131. Went PTH, Lugli A, Meier S, Bundi M, Mirlacher M, Sauter G, Dirnhofer S. *Hum. Pathol.* 2004; 35:122. [PubMed: 14745734]

132. Kang JH, Driscoll H, Mammoto A, Watters AL, Melakeberhan B, Diaz A, Super M, Ingber DE. *Adv. Biosys.* 2017; 1:1700094.
133. Hou S, Zhao L, Shen Q, Yu J, Ng C, Kong X, Wu D, Song M, Shi X, Xu X. *Angew. Chem. Int. Ed.* 2013; 52:3379.
134. Lee Y-TN. *J. Surg. Oncol.* 1983; 23:175. [PubMed: 6345937]
135. Wiseman BS, Werb Z. *Science.* 2002; 296:1046. [PubMed: 12004111]
136. Agudelo-Garcia PA, De Jesus JK, Williams SP, Nowicki MO, Chiocca EA, Liyanarachchi S, Li P-K, Lannutti JJ, Johnson JK, Lawler SE, Viapiano MS. *Neoplasia.* 2011; 13:831. [PubMed: 21969816]
137. Sims-Mourtada J, Niamat RA, Samuel S, Eskridge C, Kmiec EB. *Int. J. Nanomedicine.* 2014; 9:995. [PubMed: 24570583]
138. Fidler IJ. *Differentiation.* 2002; 70:498. [PubMed: 12492492]
139. Zervantonakis IK, Hughes-Alford SK, Charest JL, Condeelis JS, Gertler FB, Kamm RD. *Proc. Natl. Acad. Sci. USA.* 2012; 109:13515. [PubMed: 22869695]
140. a) Szot CS, Buchanan CF, Freeman JW, Rylander MN. *Biomaterials.* 2011; 32:7905. [PubMed: 21782234] b) Loessner D, Stok KS, Lutolf MP, Hutmacher DW, Clements JA, Rizzi SC. *Biomaterials.* 2010; 31:8494. [PubMed: 20709389]
141. Zhang X, Wang W, Yu W, Xie Y, Zhang X, Zhang Y, Ma X. *Biotechnol. Prog.* 2005; 21:1289. [PubMed: 16080713]
142. Chen S, Liu B, Carlson MA, Gombart AF, Reilly DA, Xie J. *Nanomedicine.* 2017; 12:1335. [PubMed: 28520509]
143. a) Chew SY, Wen J, Yim EKF, Leong KW. *Biomacromolecules.* 2005; 6:2017. [PubMed: 16004440] b) Jiang J, Chen G, Shuler FD, Wang C-H, Xie J. *Pharm. Res.* 2015; 32:2851. [PubMed: 25773720]
144. Rangaswami H, Bulbule A, Kundu GC. *Trends in cell biology.* 2006; 16:79. [PubMed: 16406521]
145. Fong ELS, Lamhamedi-Cherradi S, Burdett E, Ramamoorthy V, Lazar AJ, Kasper FK, Farach-Carson MC, Vishwamitra D, Demicco EG, Menegaz BA, Amin HM, Mikos AG, Ludwig JA. *Proc. Natl. Acad. Sci. USA.* 2013; 10:6500.
146. Bates RC, Edwards NS, Yates JD. *Crit. Rev. Oncol. Hemat.* 2000; 36:61.
147. Chitcholtan K, Sykes PH, Evans JJ. *J. Transl. Med.* 2012; 10:38. [PubMed: 22394685]
148. Jaalouk DE, Lammerding J. *Nat. Rev. Mol. Cell Biol.* 2009; 10:63. [PubMed: 19197333]
149. Weigelt B, Peterse JL, Van't Veer LJ. *Nat. Rev. Cancer.* 2005; 5:591. [PubMed: 16056258]
150. Coleman RE. *Clin. Cancer Res.* 2006; 12:6243s. [PubMed: 17062708]
151. Wirtz D, Konstantopoulos K, Searson PC. *Nat. Rev. Cancer.* 2011; 11:512. [PubMed: 21701513]
152. Roodman GD. *N. Engl. J. Med.* 2004; 350:1655. [PubMed: 15084698]
153. a) Zhang J-H, Tang J, Wang J, Ma W, Zheng W, Yoneda T, Chen J. *Int. J. Oncol.* 2003; 23:1043. [PubMed: 12963984] b) Hotte SJ, Winquist EW, Stitt L, Wilson SM, Chambers AF. *Cancer.* 2002; 95:506. [PubMed: 12209742]
154. Thibaudeau L, Taubenberger AV, Holzapfel BM, Quent VM, Fuehrmann T, Hesami P, Brown TD, Dalton PD, Power CA, Hollier BJ, Hutmacher DW. *Dis. Model. Mech.* 2014; 7:299. [PubMed: 24713276]
155. Xie J, Li X, Xia Y. *Macromol. Rapid Commun.* 2008; 29:1775. [PubMed: 20011452]
156. Do A-V, Khorsand B, Geary SM, Salem AK. *Adv. Healthcare Mater.* 2015; 4:1742.
157. Lee SJ, Heo DN, Park JS, Kwon SK, Lee JH, Lee JH, Kim WD, Kwon IK, Park SA. *Phys. Chem. Chem. Phys.* 2015; 17:2996. [PubMed: 25557615]
158. Delaney G, Jacob S, Featherstone C, Barton M. *Cancer.* 2005; 104:1129. [PubMed: 16080176]
159. Ning S, Yu N, Brown DM, Kanekal S, Knox SJ. *Radiother. Oncol.* 1999; 50:215. [PubMed: 10368046]
160. Mundy GR. *Nat. Rev. Cancer.* 2002; 2:584. [PubMed: 12154351]
161. Watson AL, Carlson DF, Largaespada DA, Hackett PB, Fahrenkrug SC. *Frontiers in genetics.* 2016; 7:78. [PubMed: 27242889]
162. Ryan DP, Hong TS, Bardeesy N. *N. Engl. J. Med.* 2014; 371:1039. [PubMed: 25207767]



163. Fischer R, Breidert M, Keck T, Makowiec F, Lohrmann C, Harder J, Saudi J. *Gastroenterol.* 2012; 18:118. [PubMed: 22421717]
164. Garrido-Laguna I, Hidalgo M. *Nat. Rev. Clin. Oncol.* 2015; 12:319. [PubMed: 25824606]
165. Olive KP, Jacobetz MA, Davidson CJ, Gopinathan A, McIntyre D, Honess D, Madhu B, Goldgraben MA, Caldwell ME, Allard D, Frese KK, DeNicola G, Feig C, Combs C, Winter SP, Ireland-Zecchini H, Reichelt S, Howat WJ, Chang A, Dhara M, Wang L, Rückert F, Grützmann R, Pilarsky C, Izeradjene K, Hingorani SR, Huang P, Davies SE, Plunkett W, Egorin M, Hruban RH, Whitebread N, McGovern K, Adams J, Iacobuzio-Donahue C, Griffiths J, Tuveson DA. *Science.* 2009; 324:1457. [PubMed: 19460966]

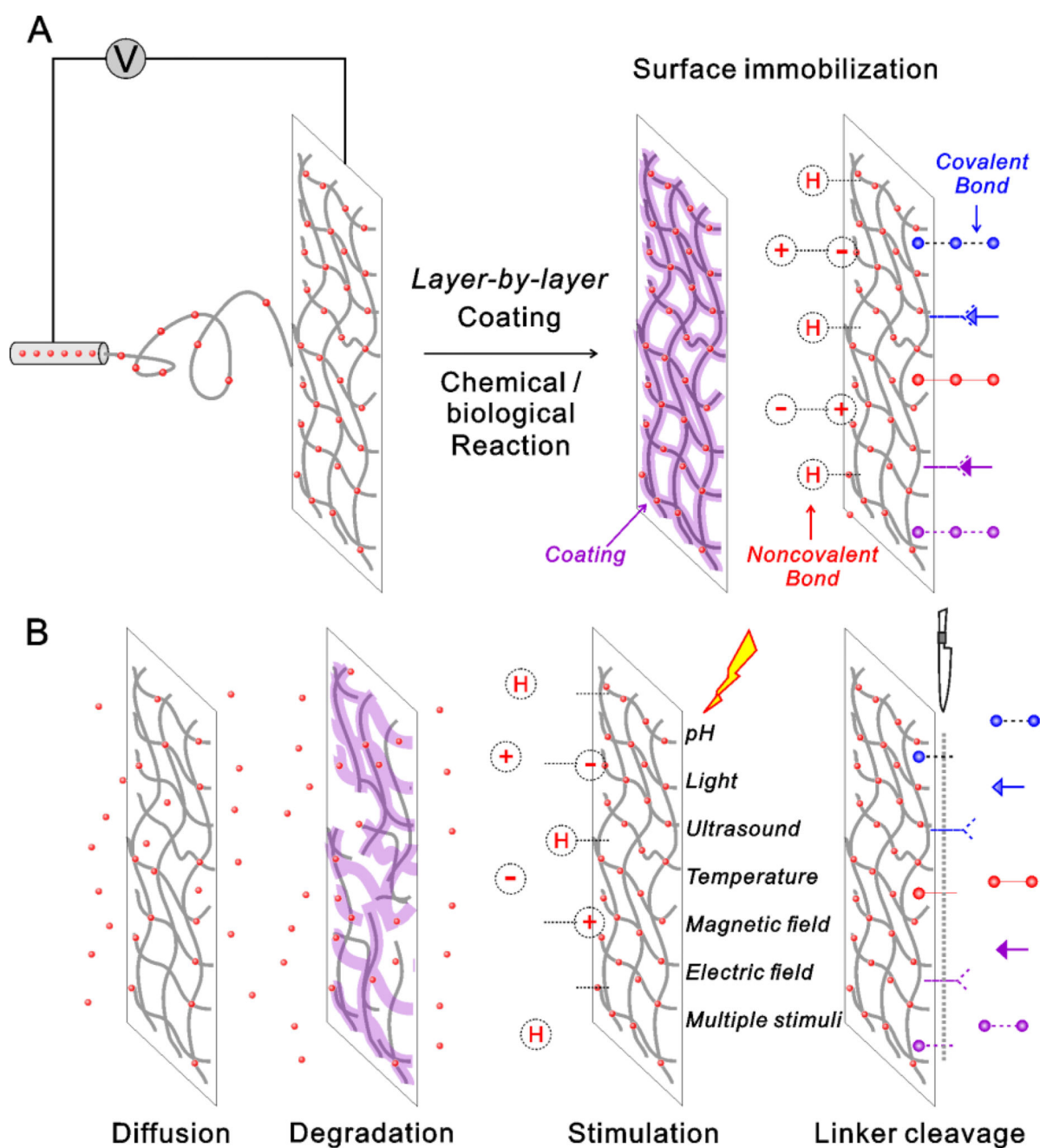


**Figure 1. Loading and release of therapeutic agents from electrospun nanofibers**  
Schematic illustrating different loading methods of therapeutic agents to electrospun fibers (A) and their corresponding release mechanisms (B).

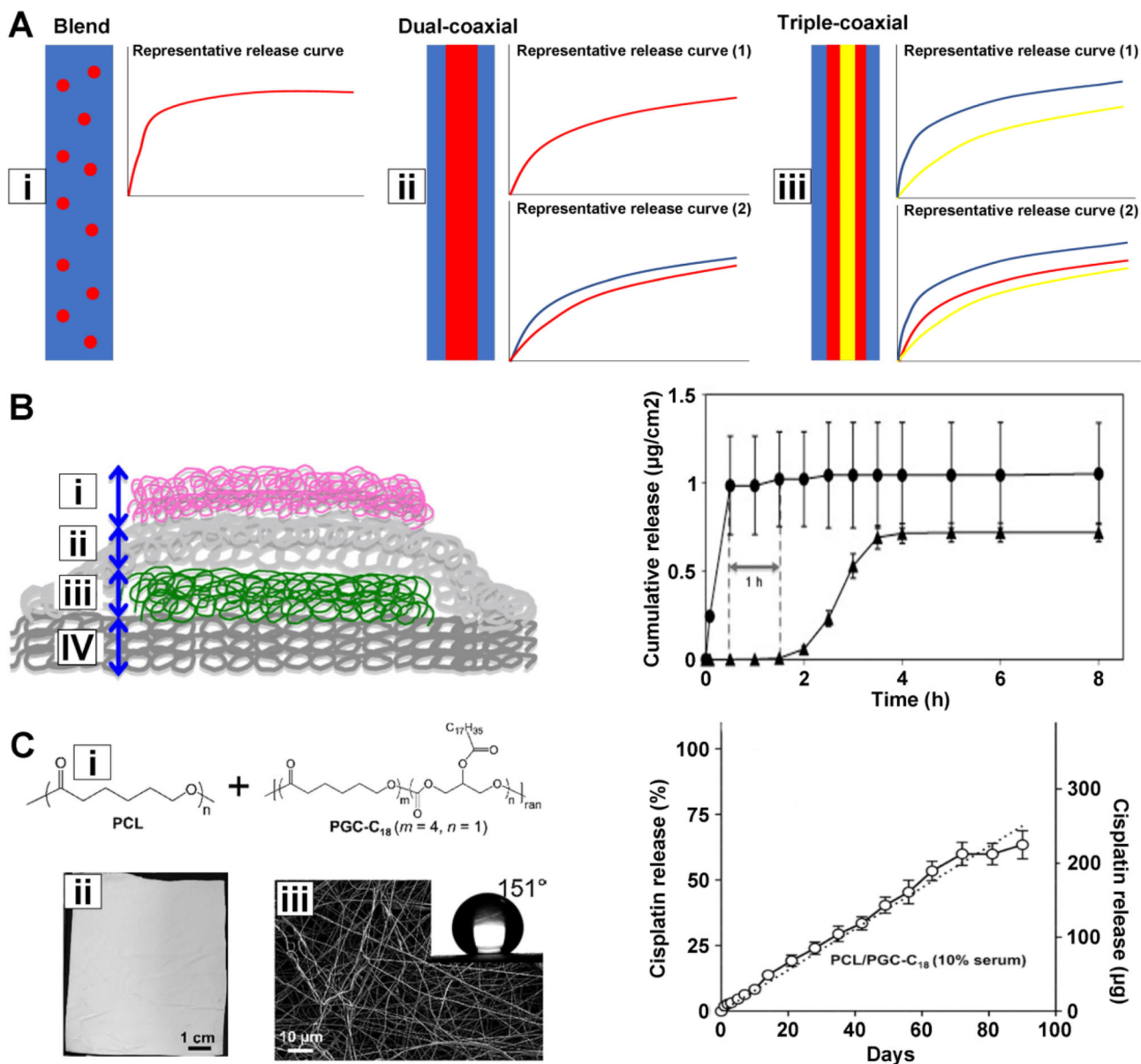


**Figure 2. Electrospun nanofibers for controlled release**

(A) Microstructures of fibers: solid, co-axial, tri-axial, and their representative release curve.

(B) Multilayered drug-loaded nanofiber meshes enable time-programmed dual release.

Reproduced with permission.<sup>[71]</sup> Copyright 2010, Elsevier. (C) Composition: additives of hydrophobic or hydrophilic materials. The additive of poly(glycerol monostearate-*co*-ε-caprolactone) (PGC-C<sub>18</sub>) (a hydrophobic material) can greatly prolong the release of drugs from PCL nanofibers. Reproduced with permission.<sup>[28b]</sup> Copyright 2016, Elsevier.

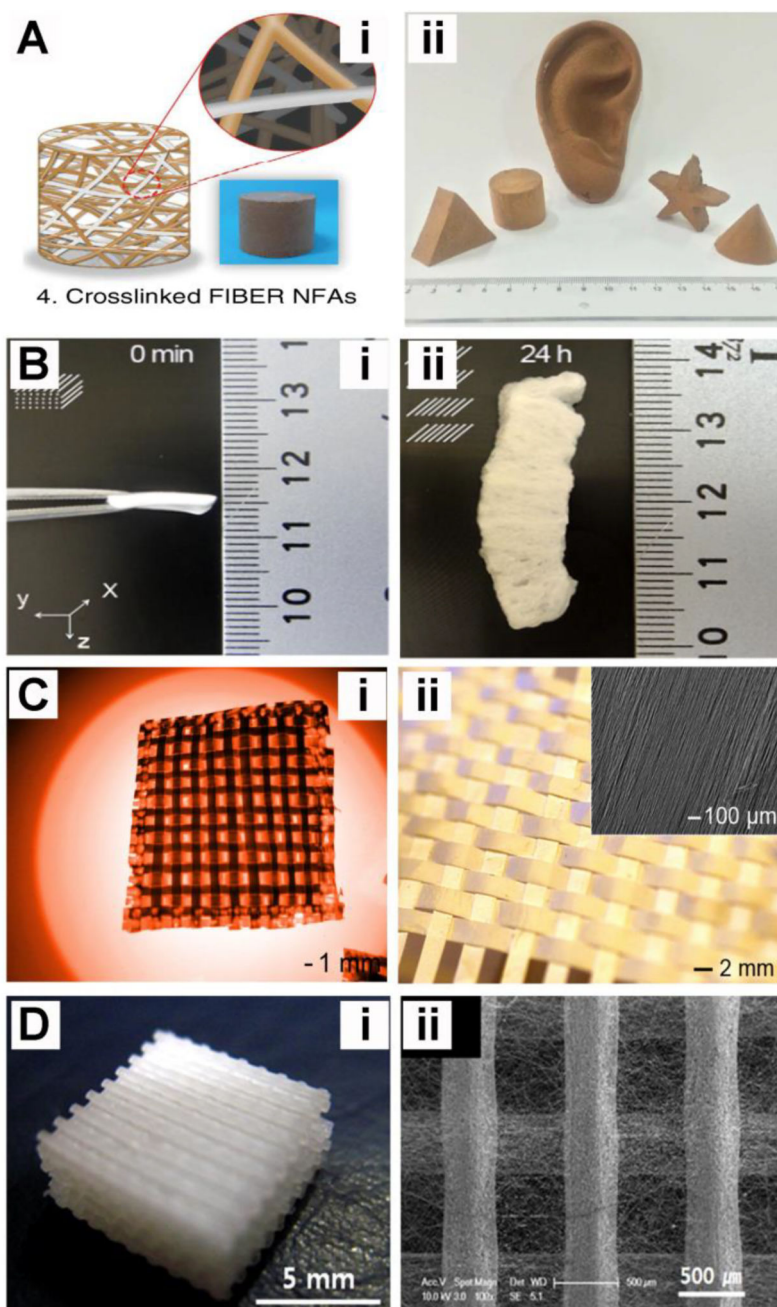


**Figure 3. Representative 3D nanofiber scaffolds generated by electrospinning**

(A) (i) Electrospun nanofiber assembled 3D scaffolds, (ii) An optical photograph of 3D scaffolds with diverse shapes. Reproduced with permission.<sup>[109]</sup> Copyright 2014, Nature Publishing Group. (B) Photographs show the PCL electrospun nanofiber before (i) and after (ii) expansion in 1M NaBH<sub>4</sub> for 24h. Reproduced with permission.<sup>[112]</sup> Copyright 2015, American Chemical Society. (C) Micrographs shows a 3D nanofiber scaffold composed of 15 layers of fiber stripes with basket-weaved structure and regular pores (i) and a 3D nanofiber scaffold composed of 2 layers of fiber stripes (ii). Reproduced with permission.<sup>[114]</sup> Copyright 2012, Wiley. (D) (i) Photograph of the overall 3D hybrid scaffolds

containing microfibers and electrospun nanofibers with dimensions of  $9\text{ mm} \times 9\text{ mm} \times 3.5\text{ mm}$ , (ii) the hybrid basic unit layer composed of microfibers and the electrospun nanofibers matrix. Reproduced with permission.<sup>[115]</sup> Copyright 2008, Elsevier.

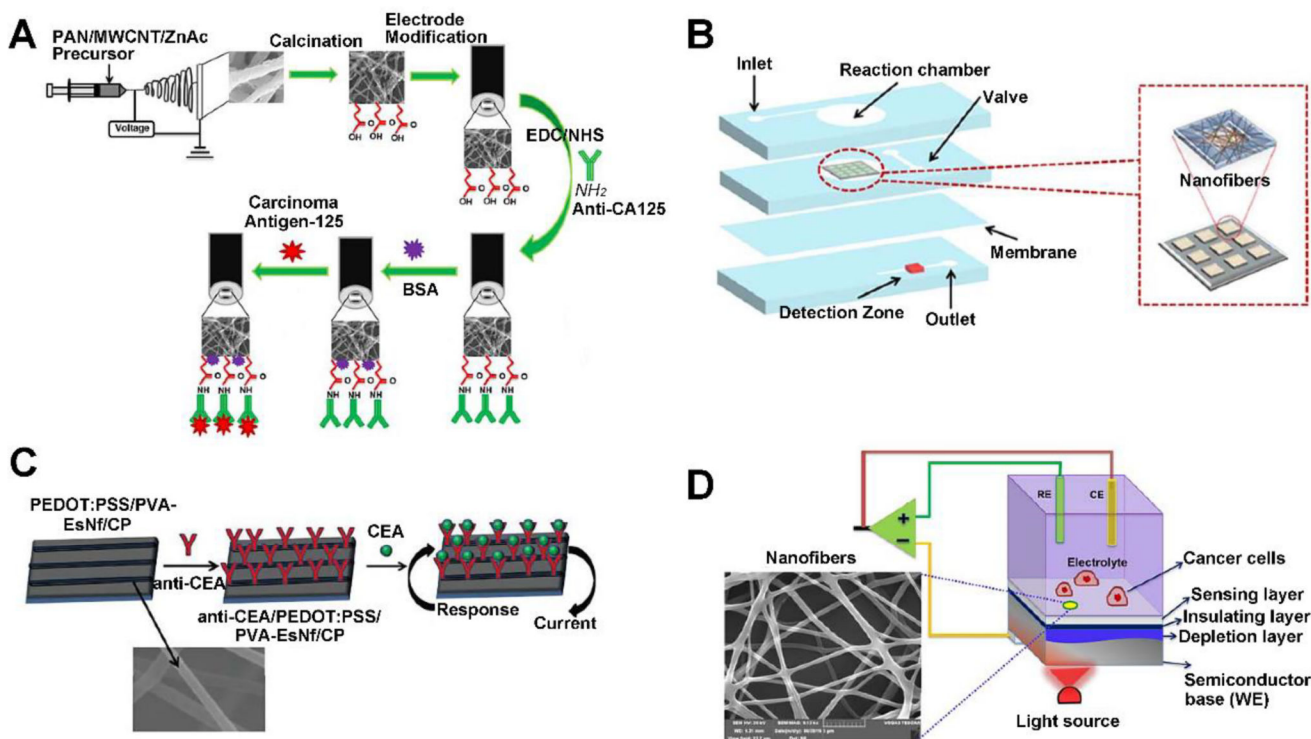


**Figure 4. Electrospun nanofibers for cancer cell detection and sensing**

(A) Schematic representation of the fabrication of biofunctionalized electrospun multiwalled carbon nanotubes embedded zinc oxide nanowire interface for highly sensitive detection of carcinoma antigen-125. Reproduced with permission.<sup>[20]</sup> Copyright 2017, Elsevier. (B) Design of the MMP-9 detecting microfluidic device integrating a hydrogel-framed electrospun nanofiber matrix. Reproduced with permission.<sup>[122]</sup> Copyright 2016, American Chemical Society. (C) Schematic representation of the biofunctionalized electrospun PEDOT:PSS/PVA nanofiber for carcinoembryonic antigen (CEA) detection.<sup>[102]</sup> (D) Schematic representation of a light addressable potentiometric sensor integrated with pH sensitive hydrogel nanofibers for measuring cancer cell metabolism and their response to anticancer drugs in real time. Reproduced with permission.<sup>[123]</sup> Copyright 2017, American Chemical Society.



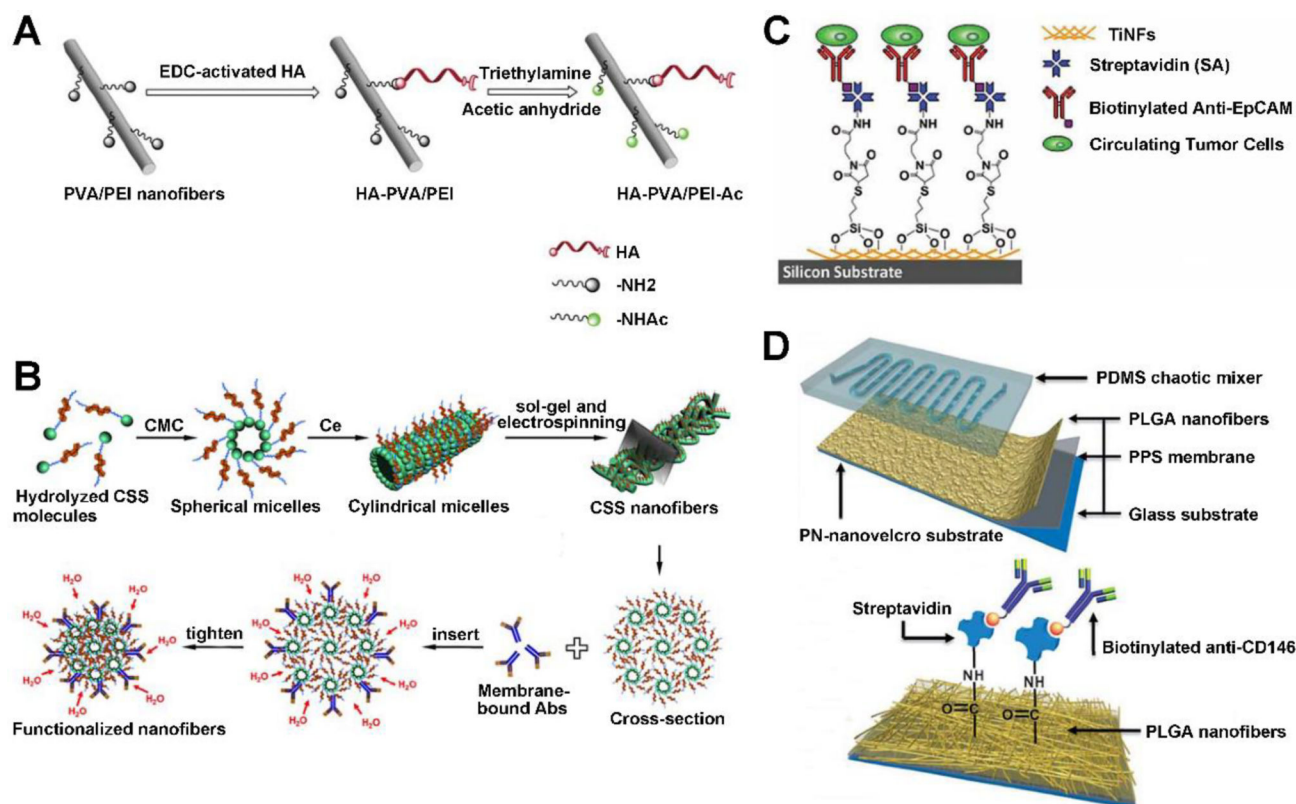


**Figure 5. Electrospun nanofibers for cancer cell capture**

(A) Schematic representation of the formation of hyaluronic acid immobilized electrospun polyvinyl alcohol/polyethyleneimine (PVA/PEI) nanofibers for capturing circulating tumor cells. Reproduced with permission.<sup>[103]</sup> Copyright 2015, Wiley. (B) Schematic representation of immobilization of membrane-bound molecules on organic-inorganic cholesteryl-succinyl silane nanofibers for capturing Granta-22 cells. Reproduced with permission.<sup>[130]</sup> Copyright 2012, AIP Publishing LLC. (C) Schematic representation of biotinylated epithelial-cell adhesion-molecule antibody (Anti-EpCAM) grafted TiO<sub>2</sub> electrospun nanofibers for colorectal and gastric cancer cell capture. Reproduced with permission.<sup>[22]</sup> Copyright 2012, Wiley. (D) Schematic representation of poly(lactic-co-glycolic acid) (PLGA)-nanofiber embedded nanovelcro chip for capturing circulating tumor cells.

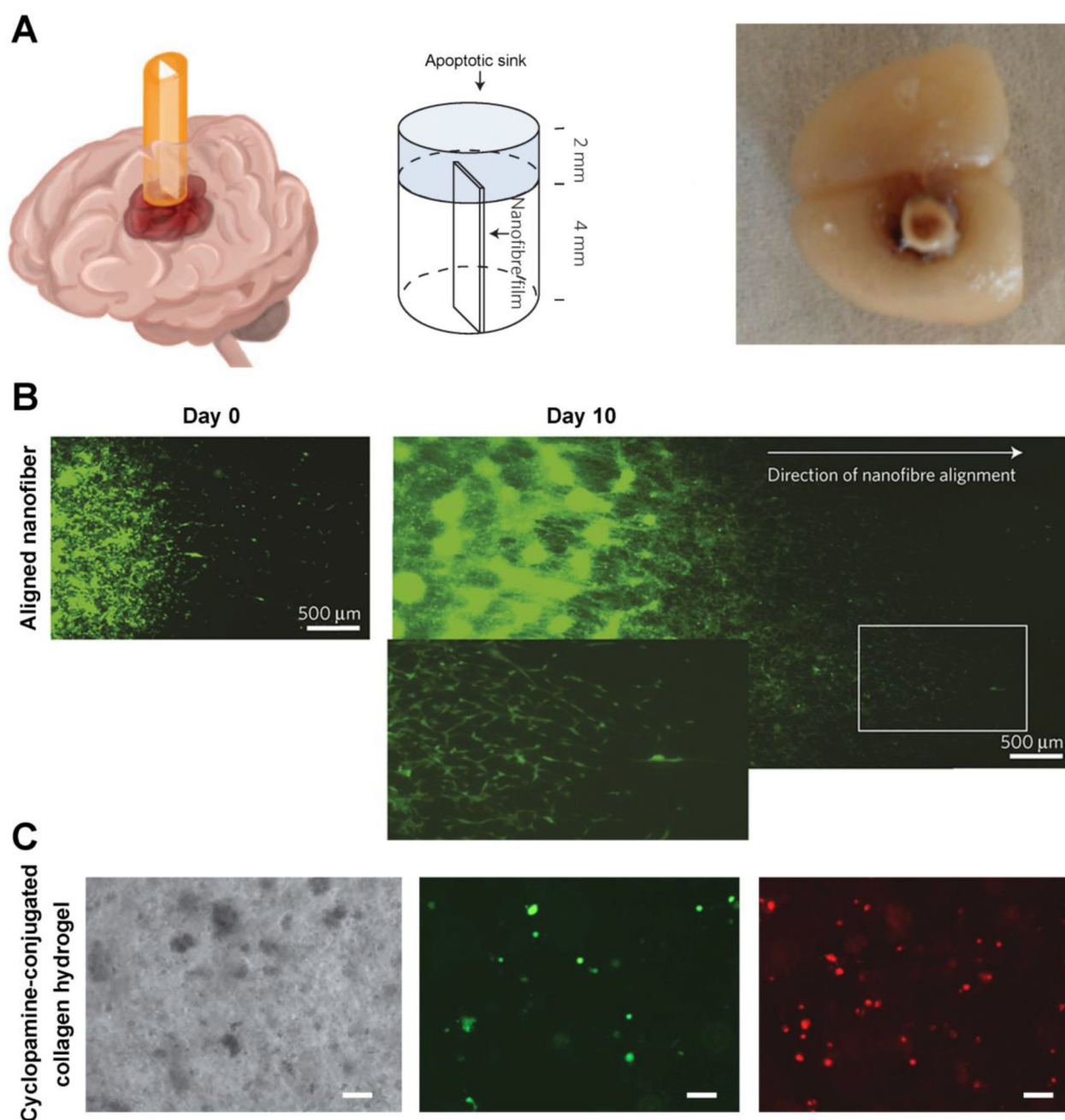


**Figure 6. Electrospun nanofibers for regulating cell behavior**

(A) Schematic and image of 'tumor guide' device inserted into a rat brain, three-dimensional view (left), 'tumor guide' device view (middle) of the brain and device, and digital image of extracted brain containing a conduit from the top view (right). (B) Fluorescence images of the tumor cells at day 0 and day 10 on the aligned nanofiber films. The cells migrated further on the aligned nanofiber film. (C) The glioblastoma cells were effectively introduced to apoptosis by cyclopamine released from collagen hydrogel after they were 'fishing' out. Reproduced with permission.<sup>[23]</sup> Copyright 2014, Nature Publishing Group.

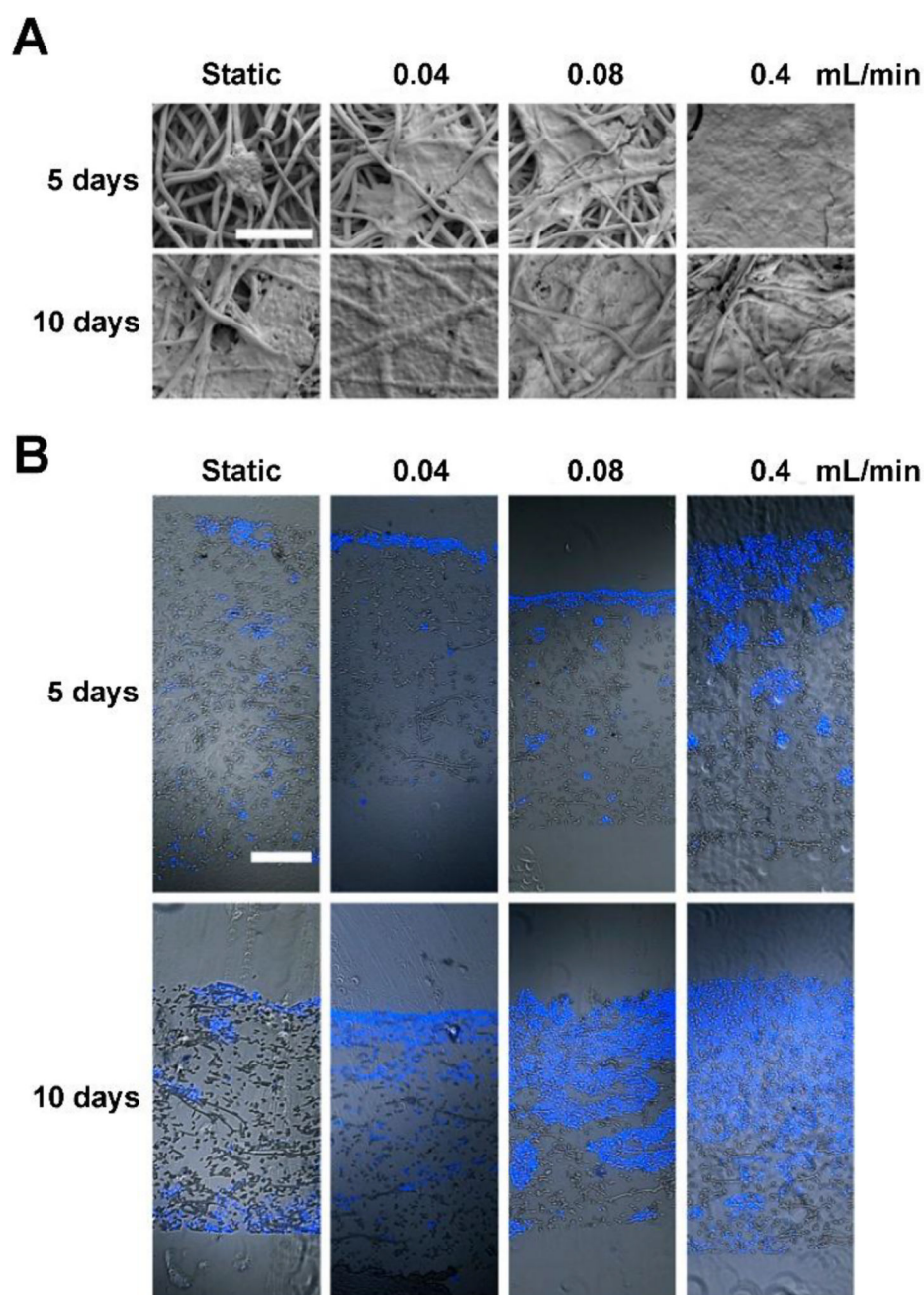


**Figure 7. Electrospun nanofibers for engineering 3D cancer models**

Effect of flow perfusion on ewing sarcoma cell morphology and distribution in a 3D electrospun PCL nanofiber cancer model. (A) SEM micrographs of the surface of scaffolds for the different flow. Scale bar is equivalent to 100  $\mu\text{m}$  in all micrographs. (B) Fluorescence microscopy of the cross section of scaffolds. Bright field images of scaffold fibers are overlapped with ewing sarcoma cells fluorescently stained with DAPI (blue staining). (Scale bar, 200  $\mu\text{m}$ ) Reproduced with permission.<sup>[101]</sup> Copyright 2015, PNAS.



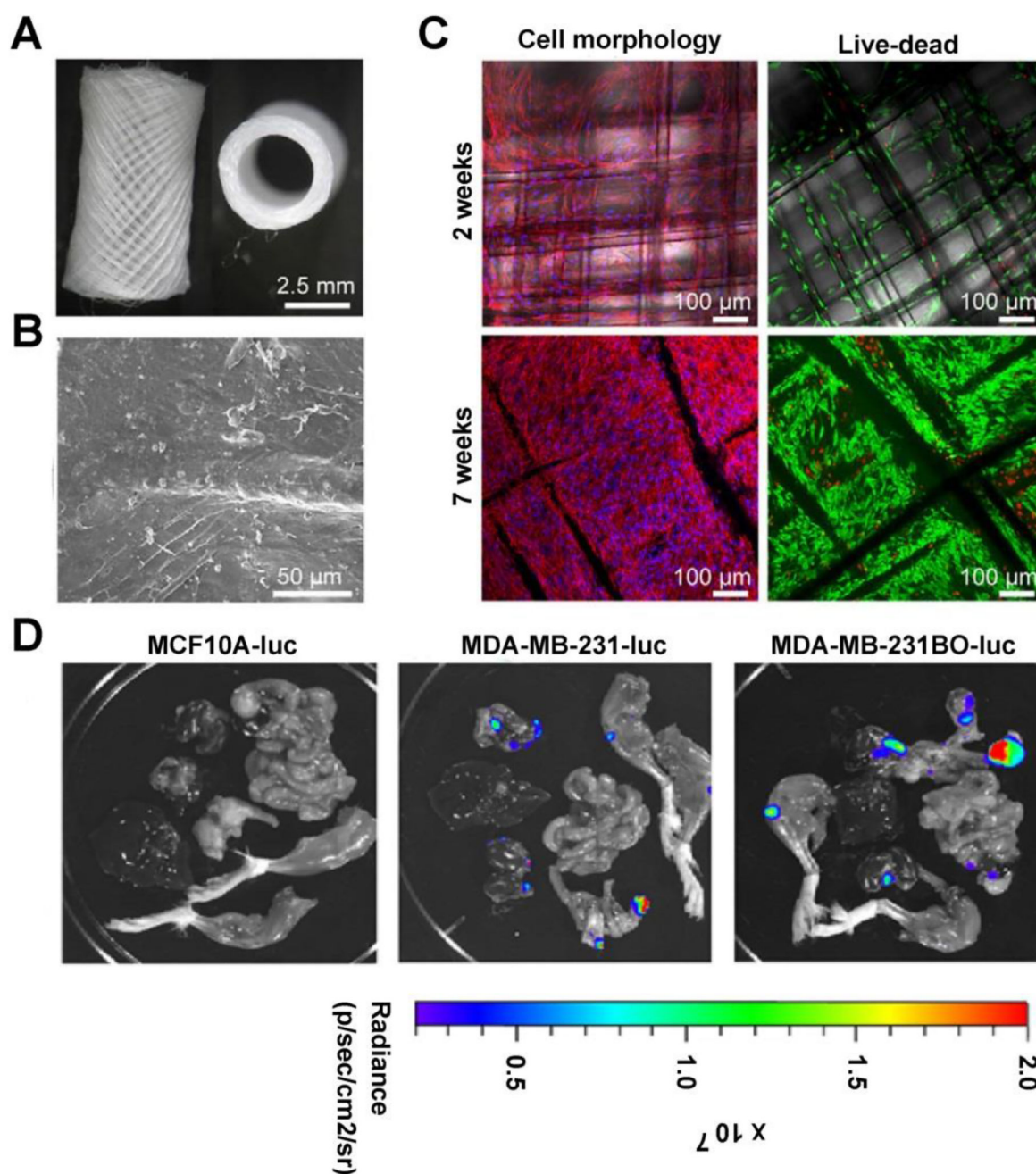


**Figure 8. Electrospun nanofibers for engineering the pre-metastatic niche**

Engineering bone tissue made by melt electrospinning for cancer metastasis study. (A) Representative images of the melt electrospun PCL scaffolds. (B) Characterization of the CaP-coated scaffolds by SEM after human osteoblastic cells seeding for 7 weeks *in vitro*. (C) Morphology and viability of the human osteoblastic cells cultured on the scaffolds is assessed by CLSM on cells stained respectively for F-actin (red) and nuclei (blue), or with markers for live (fluorescein diacetate, green) and dead (propidium iodide, red) cells after 2 and 7 weeks of culture *in vitro*. (D) Images of metastases detected by *ex vivo*

bioluminescence imaging in the tissue engineered bone and mice organs. Reproduced with permission.<sup>[154]</sup> Copyright 2014, The Company of Biologists.

Author Manuscript

Author Manuscript

Author Manuscript

Author Manuscript

**Table 1**

Representative anticancer drug, gene, and virus encapsulation into electrospun nanofibers with varied polymer compositions.

Drug	Carrier	Loading method	Type of cancer	Refs
CPT11, SN-38	PCL/PGC-C18	Encapsulation	Colorectal cancer	[27]
Cisplatin	PEO/PLA; PCL/PGC-C18	Encapsulation	Cervical cancer; lung cancer	[28]
Doxorubicin	Chitosan/PLA; PLGA/HAP; PLA/mesoporous silica nanoparticles; poly(NIPAAm- <i>co</i> -HMAAm); silica nanoparticles-DOX-CaCO <sub>3</sub> /PLLA; polydopamine/PCL; gelatin/PCL-PEG micelle;	Encapsulation Immobilization	Graffi myeloid tumor; epithelial carcinoma; orthotopic secondary hepatic carcinoma; postsurgical cancer; skin cancer; HeLa cells; H1299 cells; breast cancer	[29]
Doxorubicin and camptothecin	PLGA/gelatin/ZnO nanospheres	Encapsulation	Liver cancer	[30]
Paclitaxel	PLGA; Chitosan/PEO	Encapsulation	Glioma; prostate cancer	[31]
Paclitaxel and doxorubicin	PEG-PLA	Encapsulation	Glioma	[32]
5-aminolevulinic acid	PVA	Encapsulation	Cholangiocarcinoma	[33]
Hydroxycamptothecin	PEG-PDLA	Encapsulation	Hepatoma	[34]
Combretastatin A-4 and hydroxycamptothecin	PEG-PLA	Encapsulation	Breast cancer	[35]
Titanocene dichloride	PLLA	Encapsulation	Lung cancer	[36]
Temozolomide	PLGA/PLA/PCL	Encapsulation	Glioma	[15]
1,3-bis(2-chloroethyl)-1-nitrosourea	PEG-PLLA	Encapsulation	Glioma	[37]
Green tea polyphenols	PCL/MWCNTs	Encapsulation	Lung cancer and liver cancer	[38]
Curcumin	PCL-PEG-PCL; PLGA	Encapsulation	Glioma; skin	[39]
Daunorubicin	Poly(N-isopropylacrylamide)- <i>co</i> -polystyrene;	Encapsulation	Leukemia	[40]
Daunorubicin and Fe <sub>3</sub> O <sub>4</sub> nanoparticles	PLA	Encapsulation	Leukemia	[41]
Cdk2 siRNA	plasmid DNA/PCL	Encapsulation	Breast cancer	[42]
MMP-2 RNAi and Paclitaxel	PEI/DNA nanoparticles/PLGA	Encapsulation	brain tumor	[43]
Inactivated sendai virus	PCL	Surface immobilization	Prostate cancer	[44]
Fe <sub>3</sub> O <sub>4</sub> nanoparticles	Chitosan	Surface immobilization	Colon adenocarcinoma	[45]



**Table 2**

Electrospun nanofiber-based biosensors for cancer cell detection.

Materials	Type of sensing	Type of interaction	Sensitivity	Refs
Multiwalled carbon nanotubes (MWCNT) embedded ZnO nanofibers	Detection of carcinoma antigen-125	Antigen/antibody interaction	90.14 $\mu\text{A}/(\text{U}/\text{mL})/\text{cm}^2$	[20]
Graphene foam modified with electrospun carbon-doped $\text{TiO}_2$ nanofibers	Detection of breast cancer biomarker EGFR2, ErbB2	Antigen/antibody interaction	0.585 $\mu\text{A}/\mu\text{M}/\text{cm}^2$	[121]
PS/PSMA nanofibers	Detection of matrix metalloproteinases (MMPs)	Specific interaction between enzyme (MMPs) and substrate (peptides)	10 pM	[122]
Mesoporous zinc oxide nanofibers	Detection of breast cancer biomarker EGFR2, ErbB2	Antigen/antibody interaction	7.76 $\text{k}\Omega/\mu\text{M}$ ; 1 fM ( $4.34 \times 10^{-5} \text{ ng/mL}$ )	[125]
PEDOT:PSS/PVA nanofibers	Detection of carcinoembryonic antigen	Antigen/antibody interaction	14.2 $\mu\text{A}/\text{ng mL}/\text{cm}^2$	[102]
PVA/PAA nanofibers	Detection of pH changes	pH response	74 mV/pH	[123]
Core/shell fibers with PCL as shell and Ru(dpp) and PtOEP containing PDMS as the core	Oxygen detection	Oxygen response	Response less than 0.5 s	[124]